

Stability Analysis of Newton-MR Under Hessian Perturbations

Yang Liu* Fred Roosta†

April 13, 2022

Abstract

Recently, stability of Newton-CG under Hessian perturbations, i.e., inexact curvature information, have been extensively studied. Such stability analysis has subsequently been leveraged in designing variants of Newton-CG in which, to reduce the computational costs involving the Hessian matrix, the curvature is suitably approximated. Here, we do that for Newton-MR, [48], which extends Newton-CG in the same manner that MINRES extends CG. Unlike the stability analysis of Newton-CG, which relies on spectrum preserving perturbations in the sense of Löwner partial order, our work here draws from matrix perturbation theory to estimate the distance between the underlying exact and perturbed sub-spaces. Numerical experiments demonstrate great degree of stability for Newton-MR, amounting to a highly efficient algorithm in large-scale problems.

1 Introduction

Consider the unconstrained optimization problem:

$$\min_{\mathbf{x} \in \mathbb{R}^d} f(\mathbf{x}), \quad (1)$$

where $f : \mathbb{R}^d \rightarrow \mathbb{R}$. Due to simplicity and solid theoretical foundations, there is an abundance of algorithms designed specifically for the case where f is convex [5, 8, 42]. Strong-convexity, as a special case, allows for the design of algorithms with great many theoretical and algorithmic properties.

In such settings, the classical Newton’s method and its Newton-CG variant hold a special place. In particular, for strongly-convex functions with sufficient degree of smoothness, they have been shown to enjoy various desirable properties including insensitivity to problem ill-conditioning [49, 64], problem-independent local convergence

*School of Mathematics and Physics, University of Queensland, Australia. Email: yang.liu2@uq.edu.au

†School of Mathematics and Physics, University of Queensland, Australia, and International Computer Science Institute, Berkeley, USA. Email: fred.roosta@uq.edu.au

rates [50], and robustness to hyper-parameter tuning [3, 35]. Arguably, the only drawback of Newton’s method in large-scale problems is the computational costs involving the application of the Hessian matrix. In this light, several recent efforts have focused on the design and analysis of variants of the classical Newton’s method and its Newton-CG variant, in which the exact Hessian matrix, $\mathbf{H} \triangleq \nabla^2 f(\mathbf{x})$ is replaced with its suitable approximation $\tilde{\mathbf{H}} \approx \nabla^2 f(\mathbf{x})$; see for example [7, 9, 10, 27, 47, 50, 64]. At the heart of these efforts lies stability analysis of Newton’s method with respect to Hessian perturbations

$$\tilde{\mathbf{H}} = \mathbf{H} + \mathbf{E}, \tag{2a}$$

for some symmetric matrix \mathbf{E} , and to determine bounds

$$\|\mathbf{E}\| \leq \epsilon, \tag{2b}$$

such that the algorithm with inexact Hessian maintains, to a great extent, its original convergence properties using the exact curvature information.

However, in the absence of either sufficient smoothness or strong-convexity, the classical Newton’s method and its Newton-CG can simply break down, e.g., their underlying sub-problems may fail to have a solution. Hence, many Newton-type variants have been proposed which aim at extending Newton’s method beyond strongly convex problems, e.g., Levenberg-Marquardt [37, 38], trust-region [22], cubic regularization [15, 16, 43], and various other methods, which make clever use of negative curvature when it arises [13, 14, 52, 53]. Variants of these methods using inexact function approximations, including approximate Hessian, have also been studied, e.g., [2, 6, 17, 18, 23, 31, 36, 55, 63, 65]. However, many of these methods rely on strict smoothness assumptions such as Lipschitz continuity of gradient and Hessian. In addition, in sharp contrast to Newton’s method whose sub-problems are simple linear systems, a vast majority of these methods involve sub-problems that are themselves non-trivial to solve, e.g., the sub-problems of trust-region and cubic regularization methods are non-linear and non-convex.

To extend the application range of the classical Newton’s method beyond strongly convex settings, while maintaining the simplicity of its sub-problems, Newton-MR [48] has recently been proposed. On the surface, Newton-MR bares a striking resemblance to the classical Newton’s method and shares several of its desirable properties, e.g., Newton-MR involves simple sub-problems in the form of ordinary least squares. However, Newton-MR can be readily applied to a class of non-convex problems known as invex [41], which subsumes convexity as a sub-class. Furthermore, its required smoothness assumptions are more relaxed as compared with most non-convex Newton-type methods. Motivated by the potential and advantages of Newton-MR, in this paper we provide its stability analysis with respect to Hessian perturbations. In this light, we show that appropriately approximating the Hessian matrix allows for efficient application of Newton-MR to large-scale problems.

The rest of this paper is organized as follows. We end this section by introducing the notation used throughout this paper. In Section 2, we briefly review Newton-MR and, in its light, introduce the variant in which the Hessian is perturbed. Stability analysis of the resulting algorithm is gathered in Section 3. Numerical experiments

demonstrating the performance of Newton-MR as compared with several first and second order methods are presented in Section 4. Conclusions are gathered in Section 5.

Notation Throughout the paper, vectors and matrices are denoted by bold lower-case and bold upper-case letters, respectively, e.g., \mathbf{v} and \mathbf{V} . We use regular lower-case and upper-case letters to denote scalar constants, e.g., d or L . For a real vector, \mathbf{v} , its transpose is denoted by \mathbf{v}^\top . For two vectors \mathbf{v}, \mathbf{w} , their inner-product is denoted as $\langle \mathbf{v}, \mathbf{w} \rangle = \mathbf{v}^\top \mathbf{w}$. For a vector \mathbf{v} and a matrix \mathbf{V} , $\|\mathbf{v}\|$ and $\|\mathbf{V}\|$ denote vector ℓ_2 norm and matrix spectral norm, respectively. Iteration counter for the main algorithm appears as subscript, e.g., \mathbf{p}_k . Iteration counter for sub-problem solver to obtain \mathbf{p}_k appears as superscript, e.g., $\mathbf{p}_k^{(t)}$. The vector of all zero components is denoted by $\mathbf{0}$. For two symmetric matrices \mathbf{A} and \mathbf{B} , the Löwner partial order $\mathbf{A} \succeq \mathbf{B}$ indicates that $\mathbf{A} - \mathbf{B}$ is symmetric positive semi-definite. For any $\mathbf{x}, \mathbf{z} \in \mathbb{R}^2$, $\mathbf{y} \in [\mathbf{x}, \mathbf{z}]$ denotes $\mathbf{y} = \mathbf{x} + \tau(\mathbf{z} - \mathbf{x})$ for some $0 \leq \tau \leq 1$. \mathbf{A}^\dagger denotes the Moore-Penrose generalized inverse of matrix \mathbf{A} . The element of a matrix \mathbf{A} located at the i^{th} row and the j^{th} column is denoted by $[\mathbf{A}]_{ij}$. $\sigma_i(\mathbf{A})$ denotes i^{th} largest singular values of a matrix \mathbf{A} . $\lambda_j(\mathbf{A})$ denotes j^{th} largest eigenvalue of a square matrix \mathbf{A} . For notational simplicity, we use $\mathbf{g}(\mathbf{x}) \triangleq \nabla f(\mathbf{x}) \in \mathbb{R}^d$ and $\mathbf{H}(\mathbf{x}) \triangleq \nabla^2 f(\mathbf{x}) \in \mathbb{R}^{d \times d}$ for the gradient and the Hessian of f at \mathbf{x} , respectively, and at times we drop the dependence on \mathbf{x} by simply using \mathbf{g} and \mathbf{H} , e.g., $\mathbf{g}_k = \mathbf{g}(\mathbf{x}_k)$ and $\mathbf{H}_k = \mathbf{H}(\mathbf{x}_k)$. Similarly, $\tilde{\mathbf{H}}$ denotes the perturbed Hessian. We let $r = \text{Rank}(\mathbf{H})$ and $\tilde{r} = \text{Rank}(\tilde{\mathbf{H}})$. \mathbf{U} and $\tilde{\mathbf{U}}$ are arbitrary bases for $\text{Range}(\mathbf{H})$ and $\text{Range}(\tilde{\mathbf{H}})$, respectively, and \mathbf{U}_\perp and $\tilde{\mathbf{U}}_\perp$ are their corresponding orthogonal complements. Assuming $\tilde{r} \geq r$, we let the singular value decomposition of \mathbf{H} and $\tilde{\mathbf{H}}$ be

$$\mathbf{H} = [\mathbf{U} \ \mathbf{U}_\perp] \begin{bmatrix} \Sigma & 0 \\ 0 & 0 \end{bmatrix} \mathbf{V}^\top, \quad \text{and} \quad \tilde{\mathbf{H}} = \underbrace{[\tilde{\mathbf{U}}_1 \ \tilde{\mathbf{U}}_2 \ \tilde{\mathbf{U}}_\perp]}_{\tilde{\mathbf{U}}} \begin{bmatrix} \tilde{\Sigma}_1 & 0 & 0 \\ 0 & \tilde{\Sigma}_2 & 0 \\ 0 & 0 & 0 \end{bmatrix} \tilde{\mathbf{V}}^\top, \quad (3)$$

where

$$\begin{aligned} \mathbf{U} &\in \mathbb{R}^{d \times r}, \Sigma \in \mathbb{R}^{r \times r}, \mathbf{V} \in \mathbb{R}^{d \times d}, \\ \tilde{\mathbf{U}}_1 &\in \mathbb{R}^{d \times r}, \tilde{\mathbf{U}}_2 \in \mathbb{R}^{d \times (\tilde{r} - r)}, \tilde{\Sigma}_1 \in \mathbb{R}^{r \times r}, \tilde{\Sigma}_2 \in \mathbb{R}^{(\tilde{r} - r) \times (\tilde{r} - r)}, \tilde{\mathbf{V}} \in \mathbb{R}^{d \times d}. \end{aligned}$$

Note that $\tilde{\mathbf{U}} \in \mathbb{R}^{d \times \tilde{r}}$ is divided into $\tilde{\mathbf{U}}_1 \in \mathbb{R}^{d \times r}$ and $\tilde{\mathbf{U}}_2 \in \mathbb{R}^{d \times (\tilde{r} - r)}$. Furthermore, \mathbf{U} and $\tilde{\mathbf{U}}_1$ have the same rank. Finally, ‘‘Arg min’’ implies that the minimum is attained at more than one point.

2 Newton-MR Algorithm

In non-convex settings, the Hessian matrix could be indefinite and possibly rank-deficient. In this light, at the k^{th} iteration, Newton-MR in its pure form involves the exact update direction of the form [48]

$$\mathbf{p}_k = -[\mathbf{H}_k]^\dagger \mathbf{g}_k. \quad (4)$$

The exact update direction (4) can be equivalently written as the least norm solution to the least squares problem $\|\mathbf{g}_k + \mathbf{H}_k \mathbf{p}\|$, i.e.,

$$\min_{\mathbf{p} \in \mathbb{R}^d} \|\mathbf{p}\| \quad \text{s.t.} \quad \mathbf{p} \in \underset{\hat{\mathbf{p}} \in \mathbb{R}^d}{\text{Arg min}} \|\mathbf{H}_k \hat{\mathbf{p}} + \mathbf{g}_k\|. \quad (5)$$

In practice, computing the Moore-Penrose generalized inverse can be computationally prohibitive, in which case the inexact variant of Newton-MR makes use of approximate update direction as

$$\text{Find } \mathbf{p}_k \in \text{Range}(\mathbf{H}_k), \quad \text{s.t.} \quad \langle \mathbf{p}_k, \mathbf{H}_k \mathbf{g}_k \rangle \leq -(1 - \theta) \|\mathbf{g}_k\|^2, \quad (6)$$

where $\theta < 1$ is the inexactness tolerance. It is easy to see that (6) is implied by (5). When $\mathbf{g}_k \in \text{Range}(\mathbf{H}_k)$, i.e., the linear system $\mathbf{H}_k \mathbf{p} = -\mathbf{g}_k$ is consistent, MINRES [46] can be used to obtain (approximate) pseudo-inverse solution. However, due to its many desirable properties, MINRES-QLP [19, 20] has been advocated in [48] for more general cases as the preferred solver for (5) or (6). When the Hessian is perturbed, even if initially $\mathbf{g}_k \in \text{Range}(\mathbf{H}_k)$, it is generally most likely that $\mathbf{g}_k \notin \text{Range}(\tilde{\mathbf{H}}_k)$, and hence MINRES-QLP remains the method of choice for our setting here.

After computing the update direction, the next iterate is obtained by moving along \mathbf{p}_k by some appropriate step length, i.e., $\mathbf{x}_{k+1} = \mathbf{x}_k + \alpha_k \mathbf{p}_k$. Note that from both (5) and (6) it follows that $\langle \mathbf{p}_k, \mathbf{H}_k \mathbf{g}_k \rangle \leq 0$, i.e., \mathbf{p}_k is a descent direction for the norm of the gradient, $\|\mathbf{g}\|^2$. As a result, the step-size, α_k , can be chosen by applying Armijo-type line search [1, 44] such that for some $0 < \alpha_k \leq 1$, we have

$$\|\mathbf{g}_{k+1}\|^2 \leq \|\mathbf{g}_k\|^2 + 2\rho\alpha_k \langle \mathbf{p}_k, \mathbf{H}_k \mathbf{g}_k \rangle, \quad (7)$$

where $0 < \rho < 1$ is a given line-search parameter. Typically, back-tracking strategy [44] is employed to approximately find such a step-size.

Modification of Newton-MR to include perturbed matrix $\tilde{\mathbf{H}}$ as in (2b) is rather straightforward. We simply replace \mathbf{H}_k with $\tilde{\mathbf{H}}_k$ in all of (5) to (7). The modified variant is depicted in Algorithm 1. Note that, in this context, whenever we refer to (5), (6) and (7), it is implied that $\tilde{\mathbf{H}}$ is used instead of \mathbf{H} .

Our results in this paper address the stability of Algorithm 1 with respect to Hessian perturbations of the form (2). One natural application of such stability analysis is in designing efficient variants of Newton-MR in which the Hessian, as a way to reduce computational costs, is suitably approximated.

Example 1 (Hessian Approximation in Finite-sum Minimization). Consider finite-sum optimization problems where $f(\mathbf{x}) = \frac{1}{n} \sum_{i=1}^n f_i(\mathbf{x})$ and for which, the Hessian matrix can be written as

$$\mathbf{H} = \frac{1}{n} \sum_{i=1}^n \nabla^2 f_i(\mathbf{x}). \quad (8a)$$

By considering a sample of size $|\mathcal{S}|$, we can form the sub-sampled Hessian as

$$\tilde{\mathbf{H}} = \frac{1}{|\mathcal{S}|} \sum_{j \in \mathcal{S}} \nabla^2 f_j(\mathbf{x}), \quad (8b)$$

where \mathcal{S} and $|\mathcal{S}|$ denote the sample collection and its cardinality, respectively. If the sample size is large enough, one can obtain perturbation bounds of the form (2). In the big-data regimes where $|\mathcal{S}| \ll n$, sub-sampling Hessian has been shown to result in a great deal of computational savings for a variety of Newton-type algorithms, e.g., [7, 9, 35, 51, 62, 63, 64, 65]. As an example of ways to obtain (2), Theorem 1 below, initially given in [63], establishes a sufficient bound on $|\mathcal{S}|$ for the case where samples are drawn uniformly at random. Bounds using non-uniform sampling have also been given, e.g., [63, 64]

Theorem 1 (Uniform Sub-sampling of Hessian [63]). *For any $0 < \epsilon, \delta < 1$, if $|\mathcal{S}| \in \mathcal{O}(\epsilon^{-2} \log(2d/\delta))$, we have $\Pr\left(\|\mathbf{H} - \tilde{\mathbf{H}}\| \leq \epsilon\right) \geq 1 - \delta$, where \mathbf{H} and $\tilde{\mathbf{H}}$ are defined in (8).*

In Section 4, we consider evaluating the performance of Algorithm 1 in this context.

Algorithm 1 Newton-MR With Inexact Hessian Information

- 1: **Input:** \mathbf{x}_0 , $0 < \tau < 1$, $0 < \rho < 1$
 - 2: **for** $k = 0, 1, 2, \dots$ until $\|\mathbf{g}_k\| \leq \tau$ **do**
 - 3: Solve (5) (or (6) with MINRES-QLP) with $\tilde{\mathbf{H}}_k$ in place of \mathbf{H}_k
 - 4: Find α_k such that (7) holds with $\tilde{\mathbf{H}}_k$ in place of \mathbf{H}_k
 - 5: Update $\mathbf{x}_{k+1} = \mathbf{x}_k + \alpha_k \mathbf{p}_k$
 - 6: **end for**
 - 7: **Output:** \mathbf{x} for which $\|\mathbf{g}_k\| \leq \tau$
-

3 Stability Analysis

In this section we present the stability analysis of Algorithm 1. In particular, in Section 3.2, we first gather the assumptions on the objective function. In Section 3.1, we investigate the implications of Hessian perturbation (2) as it relates to our non-convex settings here. The detailed convergence analysis of Algorithm 1 is given in Section 3.4.

3.1 Hessian Perturbations in Non-convex Settings

In strongly-convex settings, establishing the stability of the classical Newton’s method and its Newton-CG variant relies on Hessian perturbations that are *approximately spectrum preserving*, e.g., ϵ in (2) must be such that for the perturbed Hessian, we have

$$(1 - \tilde{\epsilon}_1)\mathbf{H} \preceq \tilde{\mathbf{H}} \preceq (1 + \tilde{\epsilon}_1)\mathbf{H}, \quad (9)$$

where $\tilde{\epsilon}_1 \in \mathcal{O}(\epsilon)$, e.g., [7, 27, 47, 50]. Under (9), the perturbed matrix is not only required to be full-rank, but also it must remain positive definite. In particular, (9) implies that

$$(1 - \tilde{\epsilon}_2)\mathbf{H}^{-1} \preceq \tilde{\mathbf{H}}^{-1} \preceq (1 + \tilde{\epsilon}_1)\mathbf{H}^{-1},$$

for some $\tilde{\epsilon}_2 \in \mathcal{O}(\epsilon)$, which in turn gives

$$\left\| \mathbf{H}^{-1} - \tilde{\mathbf{H}}^{-1} \right\| \leq \tilde{\epsilon}_3, \quad (10)$$

for some $\tilde{\epsilon}_3 \in \mathcal{O}(\epsilon)$ [58, Theorem 2.5], i.e., the inverse of the perturbed Hessian is itself a small perturbation of the inverse of the true Hessian.

In non-convex settings where the true Hessian might be indefinite and/or rank deficient, requiring such conditions is simply infeasible. Indeed, when \mathbf{H} is indefinite, the inequality (9) ceases to be meaningful, i.e., for no value of $\tilde{\epsilon} > 0$ we can have $(1 - \tilde{\epsilon})\mathbf{H} \preceq (1 + \tilde{\epsilon})\mathbf{H}$. Further, when \mathbf{H} has a zero eigenvalue, i.e., it is singular, it is practically impossible to assume that the corresponding eigenvalue of $\tilde{\mathbf{H}}$ is also zero. In other words, in non-convex settings, no amount of perturbation in (2) will be guaranteed to be spectrum preserving.

In non-convex settings, where the Hessian can simply fail to be invertible, one might be tempted to find a similar bound as in (10) but in terms of matrix pseudo-inverse, i.e., to find appropriate values of ϵ in (2) such that

$$\left\| \mathbf{H}^\dagger - \tilde{\mathbf{H}}^\dagger \right\| \leq \tilde{\epsilon}_3. \quad (11)$$

A cornerstone in the theory of matrix perturbations is establishing conditions on $\tilde{\mathbf{H}}$ and ϵ in (2) that can result in (11), e.g., [24, 40, 56, 58, 61]. For example, from [58, Theorem 3.8] and (2), we have

$$\left\| \mathbf{H}^\dagger - \tilde{\mathbf{H}}^\dagger \right\| \leq \left(\frac{1 + \sqrt{5}}{2} \right) \max \left\{ \left\| \mathbf{H}^\dagger \right\|^2, \left\| \tilde{\mathbf{H}}^\dagger \right\|^2 \right\} \epsilon.$$

However, employing this in our setting relies on assuming $\left\| \tilde{\mathbf{H}}^\dagger \right\| \in o(1/\sqrt{\epsilon})$, where “ $o(\cdot)$ ” denotes the “Little-O Notation”. However, as demonstrated by the following examples, this cannot be guaranteed in general.

Example 2 (Deterministic Perturbations). Suppose $\|\mathbf{E}\| = \epsilon$ and the $\text{Cond}(\mathbf{E}) \leq C$, where $\text{Cond}(\mathbf{E})$ denotes the condition number of the matrix \mathbf{E} , i.e., the ratio of its largest over its smallest non-zero singular value. This, in turn, implies $\sigma_{r_{\mathbf{E}}}(\mathbf{E}) \geq \epsilon/C$, where $\sigma_{r_{\mathbf{E}}}(\mathbf{E})$ is the smallest non-zero singular value of \mathbf{E} . Further, suppose that $r \triangleq \text{Rank}(\mathbf{H}) \leq \text{Rank}(\tilde{\mathbf{H}}) \triangleq \tilde{r}$ (cf. Lemma 2), and $r_{\mathbf{E}} = \tilde{r} + r$. By [4, Proposition 9.6.8], we have

$$\sigma_{\tilde{r}}(\tilde{\mathbf{H}}) \geq \sigma_{r_{\mathbf{E}}}(\mathbf{E}) - \sigma_{r+1}(\mathbf{H}) \geq \epsilon/C,$$

which gives $\|\tilde{\mathbf{H}}^\dagger\| \in \mathcal{O}(1/\epsilon)$.

Example 3 (Random Perturbations). Suppose $[\mathbf{E}]_{ij} \sim \mathcal{N}(0, \epsilon^2)$, where $i, j = 1, \dots, d$ and $\mathcal{N}(0, \epsilon^2)$ denotes the standard normal distribution with mean zero and standard deviation ϵ . We have $\sigma_i(\mathbf{H}) = 0$, $d \geq i > r \triangleq \text{Rank}(\mathbf{H})$. Suppose further that the non-zero singular values of \mathbf{H} are well separated from zero, e.g., $\sigma_i(\mathbf{H}) > 5\epsilon$, $i = 1, \dots, r$. Using results similar to [57, p. 411], one can show that the diagonal entries of $\tilde{\Sigma}_2$ in (3), i.e., the non-zero singular values of $\tilde{\mathbf{H}}$ corresponding to zero singular values of \mathbf{H} , will satisfy

$$\mathbb{E} \left[\sigma_i^2(\tilde{\mathbf{H}}) \right] = (d-r)\epsilon^2 \quad \text{and} \quad \sigma_i(\tilde{\mathbf{H}}) \leq \sqrt{2} \|\mathbf{E}\|, \quad i = r+1, \dots, d.$$

With probability $1 - 2\exp(-2d)$, we have $\|\mathbf{E}\| \leq 4\sqrt{d}\epsilon$ [54, Eqn (2.3), p. 1582]. The latter two inequalities alone indicate that assuming $\sigma_i(\tilde{\mathbf{H}}) \in \Omega(\sqrt{\epsilon})$, and hence the stronger condition $\|\tilde{\mathbf{H}}^\dagger\| \in o(1/\sqrt{\epsilon})$, is rather quite unreasonable. Now, on this latter event, for any $C > 1$, the reverse Markov inequality gives

$$\begin{aligned} \Pr \left(\sigma_i(\tilde{\mathbf{H}}) \leq \frac{\epsilon}{C} \right) &\leq \frac{\mathbb{E} \left[32d\epsilon^2 - \sigma_i^2(\tilde{\mathbf{H}}) \right]}{32d\epsilon^2 - \epsilon^2/C^2} \\ &\leq \frac{32d - (d-r)}{32d - 1/C^2}, \end{aligned}$$

which implies

$$\Pr \left(\sigma_i(\tilde{\mathbf{H}}) > \frac{\epsilon}{C} \right) \geq \frac{(d-r) - 1/C^2}{32d - 1/C^2}.$$

In other words, with a positive probability that is independent of ϵ , we have $\|\tilde{\mathbf{H}}^\dagger\| \in \mathcal{O}(1/\epsilon)$.

In light of the previous examples, we conduct our analysis under the following perturbation model.

Assumption 1 (Perturbation Model). *For the perturbation (2), we have*

$$\left\| \tilde{\mathbf{H}}^\dagger \right\| = \left\| [\mathbf{H} + \mathbf{E}]^\dagger \right\| \leq \frac{C}{\epsilon}, \quad (12)$$

where ϵ is as in (2) and $C \geq 1$ is some universal constant.

In any case, requiring (11) is also extremely restrictive. In fact, it is known that the necessary and sufficient condition for $\tilde{\mathbf{H}}^\dagger \rightarrow \mathbf{H}^\dagger$ as $\tilde{\mathbf{H}} \rightarrow \mathbf{H}$ is that $\tilde{\mathbf{H}}$ is an *acute perturbation* of \mathbf{H} , i.e., $\text{Rank}(\tilde{\mathbf{H}}) = \text{Rank}(\mathbf{H})$ [58, p. 146]. In other words, unless the perturbations are *rank preserving*, obtaining (11) is simply hopeless.

Consider Newton-MR with exact update as in (4). From (7), it follows that

$$\langle \mathbf{p}, \mathbf{H}\mathbf{g} \rangle = \langle \mathbf{H}\mathbf{p}, \mathbf{g} \rangle = - \left\langle \mathbf{H}\mathbf{H}^\dagger \mathbf{g}, \mathbf{g} \right\rangle = - \langle \mathbf{U}\mathbf{U}^\top \mathbf{g}, \mathbf{g} \rangle = - \|\mathbf{U}^\top \mathbf{g}\|^2,$$

where \mathbf{U} is an arbitrary orthonormal bases for $\text{Range}(\mathbf{H})$. Computing a similar quantity with $\tilde{\mathbf{H}}$ implies that, instead of (11), one could attempt at finding conditions in (2) such that

$$\left\| \mathbf{U}\mathbf{U}^\top - \tilde{\mathbf{U}}\tilde{\mathbf{U}}^\top \right\| \leq \tilde{\epsilon}_3, \quad (13)$$

where $\tilde{\mathbf{U}}$ is an orthonormal bases for $\text{Range}(\tilde{\mathbf{H}})$. In other words, at first sight, the quantity of interest could be the distance between the two subspaces, namely $\text{Range}(\mathbf{H})$ and its perturbation $\text{Range}(\tilde{\mathbf{H}})$ [29, Section 2.5.3]. More recent and improved results in bounding such distance are given in [45]. For simplicity we include the statement of [45, Theorem 19], but only slightly modified to fit the settings that we consider here.

Theorem 2 (Modified Davis-Kahan-Wedin Sine Theorem [45, Theorem 19]). *Consider a matrix $\mathbf{A} \in \mathbb{R}^{d \times d}$ of rank r , and let $\tilde{\mathbf{A}}$ be its perturbation. For an integer $1 \leq j \leq r$, let $\mathbf{U}_j \triangleq [\mathbf{u}_1, \dots, \mathbf{u}_j] \in \mathbb{R}^{d \times j}$ and $\tilde{\mathbf{U}}_j \triangleq [\tilde{\mathbf{u}}_1, \dots, \tilde{\mathbf{u}}_j] \in \mathbb{R}^{d \times j}$, where $\mathbf{u}_i \in \mathbb{R}^d$ and $\tilde{\mathbf{u}}_i \in \mathbb{R}^d$ are, respectively, i^{th} eigenvectors of matrices \mathbf{A} and $\tilde{\mathbf{A}}$. The principal angle between the sub-spaces $\text{Range}(\mathbf{U})$ and $\text{Range}(\tilde{\mathbf{U}})$ is given by*

$$\sin \angle \left(\text{Range}(\mathbf{U}), \text{Range}(\tilde{\mathbf{U}}) \right) = \left\| \mathbf{U}\mathbf{U}^\top - \tilde{\mathbf{U}}\tilde{\mathbf{U}}^\top \right\| \leq \frac{2\|\mathbf{A} - \tilde{\mathbf{A}}\|}{\sigma_j(\mathbf{A}) - \sigma_{j+1}(\mathbf{A})}. \quad (14)$$

As a result, if $\tilde{\mathbf{H}}$ is an acute perturbation of \mathbf{H} , i.e., $\text{Rank}(\tilde{\mathbf{H}}) = \text{Rank}(\mathbf{H}) = r$, we can appeal to Theorem 2 and obtain a bound as in (13). Indeed, since $\sigma_{r+1}(\mathbf{H}) = 0$ in this case, we get

$$\left\| \mathbf{U}\mathbf{U}^\top - \tilde{\mathbf{U}}\tilde{\mathbf{U}}^\top \right\| \leq \frac{2\|\mathbf{H} - \tilde{\mathbf{H}}\|}{\sigma_r(\mathbf{H})} = 2\|\mathbf{H} - \tilde{\mathbf{H}}\| \|\mathbf{H}^\dagger\| \leq 2\|\mathbf{H}^\dagger\| \epsilon.$$

However, from [4, Facts 5.12.17(iv) and 9.9.29], it simply follows that

$$\text{Rank}(\mathbf{H}) \neq \text{Rank}(\tilde{\mathbf{H}}) \implies \left\| \tilde{\mathbf{U}}\tilde{\mathbf{U}}^\top - \mathbf{U}\mathbf{U}^\top \right\| = 1.$$

Again as before, requiring (13) in non-convex settings is indeed far too stringent.

What comes to the rescue is the observation that instead of obtaining a bound as in (13), which implies a bounded distance between $\mathbf{U}\mathbf{U}^\top$ and $\tilde{\mathbf{U}}\tilde{\mathbf{U}}^\top$ along *every* direction, for Newton-MR, we only need such distance to be bounded along a *specific* direction, i.e., that of the gradient \mathbf{g} . Indeed, instead of (13), which implies

$$\left\| \left(\mathbf{H}\mathbf{H}^\dagger - \tilde{\mathbf{H}}\tilde{\mathbf{H}}^\dagger \right) \mathbf{v} \right\| \leq \tilde{\epsilon} \|\mathbf{v}\|, \quad \forall \mathbf{v} \in \mathbb{R}^d,$$

by only considering $\mathbf{v} = \mathbf{g}$ in the above, we seek to bound only the projection of the gradient on the range space of the Hessian matrices as

$$\left\| \left(\mathbf{H}\mathbf{H}^\dagger - \tilde{\mathbf{H}}\tilde{\mathbf{H}}^\dagger \right) \mathbf{g} \right\| \leq \tilde{\epsilon} \|\mathbf{g}\|, \quad \forall \mathbf{v} \in \mathbb{R}^d. \quad (15)$$

3.2 Assumptions on the Objective Function

Before presenting the stability analysis of Algorithm 1, we introduce the assumptions on the objective function f in (1) that underlie our work. We note that these assumptions are essentially the same as those in [48].

Assumption 2 (Differentiability). *The function f is twice-differentiable. In particular, all the first partial derivatives are themselves differentiable, but the second partial derivatives are allowed to be discontinuous.*

Recall that requiring the first partials be differentiable implies the equality of crossed-partials, which amounts to the symmetric Hessian matrix [33, pp. 732-733]. Note that, here, we allow Hessian to be entirely discontinuous.

Instead of the typical smoothness assumptions in the form of Lipschitz continuity of gradient and Hessian, i.e., for some $0 \leq L_{\mathbf{g}}, L_{\mathbf{H}} < \infty$

$$\|\mathbf{g}(\mathbf{x}) - \mathbf{g}(\mathbf{y})\| \leq L_{\mathbf{g}} \|\mathbf{x} - \mathbf{y}\|, \quad (16a)$$

$$\|\mathbf{H}(\mathbf{x}) - \mathbf{H}(\mathbf{y})\| \leq L_{\mathbf{H}} \|\mathbf{x} - \mathbf{y}\|, \quad (16b)$$

a more relaxed notion, called moral-smoothness, was introduced in [48].

Assumption 3 (Moral-smoothness). *For any $\mathbf{x}_0 \in \mathbb{R}^d$, there is a constant $0 < L(\mathbf{x}_0) < \infty$, such that*

$$\|\mathbf{H}(\mathbf{y})\mathbf{g}(\mathbf{y}) - \mathbf{H}(\mathbf{x})\mathbf{g}(\mathbf{x})\| \leq L(\mathbf{x}_0) \|\mathbf{y} - \mathbf{x}\|, \quad \forall (\mathbf{x}, \mathbf{y}) \in \mathcal{X}_0 \times \mathbb{R}^d, \quad (17)$$

where $\mathcal{X}_0 \triangleq \{\mathbf{x} \in \mathbb{R}^d \mid \|\mathbf{g}(\mathbf{x})\| \leq \|\mathbf{g}(\mathbf{x}_0)\|\}$.

Note that in Assumption 3, the constant $L(\mathbf{x}_0)$ depends on the choice of \mathbf{x}_0 . By (17), it is only the action of Hessian on the gradient that is required to be Lipschitz continuous, and each gradient and/or Hessian individually can be highly irregular, e.g., gradient can be very non-smooth and Hessian can even be discontinuous. In [48], it has been shown that Assumption 3 is significantly more relaxed than (16), i.e., Assumption 3 is implied by (16) and the converse is not true.

Assumption 4 (Pseudo-inverse Regularity). *There exists $\gamma > 0$, such that*

$$\|\mathbf{H}\mathbf{p}\| \geq \gamma \|\mathbf{p}\|, \quad \forall \mathbf{p} \in \text{Range}(\mathbf{H}). \quad (18)$$

Intuitively, γ is the smallest, in magnitude, among the non-zero eigenvalues of \mathbf{H} . Assumption 4 also implies that γ is required to be uniformly bounded away from zero for all \mathbf{x} ; see [48, Example 3] for examples of functions satisfying Assumption 4. Furthermore, in [48], (18) has been shown to be equivalent to

$$\|\mathbf{H}^\dagger\| \leq \frac{1}{\gamma}. \quad (19)$$

Assumption 5 (Gradient-Hessian Null-space Property). *For any $\mathbf{x} \in \mathbb{R}^d$, let \mathbf{U} and \mathbf{U}_\perp denote arbitrary orthogonal bases for $\text{Range}(\mathbf{H}(\mathbf{x}))$ and its orthogonal complement, respectively. A function is said to satisfy the Gradient-Hessian Null-Space property, if there exists $0 < \nu \leq 1$, such that*

$$\|\mathbf{U}_\perp^\top \mathbf{g}(\mathbf{x})\|^2 \leq \left(\frac{1-\nu}{\nu}\right) \|\mathbf{U}^\top \mathbf{g}(\mathbf{x})\|^2, \quad \forall \mathbf{x} \in \mathbb{R}^d. \quad (20)$$

Assumption 5 ensures that the angle between the gradient and the range-space of the Hessian matrix is uniformly bounded away from zero. In other words, as iterations progress, the gradient will not become arbitrarily orthogonal to the range space of Hessian. Explicit examples of functions that satisfy this assumption, including the special case when $\nu = 1$, i.e., the gradient lies fully in the range of the full Hessian, are given in [48]. The following lemma, also from [48, Lemma 4], is a direct consequence of Assumption 5.

Lemma 1 ([48, Lemma 4]). *Under Assumption 5, we have*

$$\|\mathbf{U}^\top \mathbf{g}\|^2 \geq \nu \|\mathbf{g}\|^2, \quad (21a)$$

$$\|\mathbf{U}_\perp^\top \mathbf{g}\|^2 \leq (1-\nu) \|\mathbf{g}\|^2. \quad (21b)$$

3.3 Perturbation Analysis

Although assuming rank-preserving perturbation, i.e., $\text{Rank}(\mathbf{H}_k) = \text{Rank}(\tilde{\mathbf{H}}_k)$, is too stringent to be of any practical use, under certain conditions, we can ensure that the perturbed matrix has a rank at least as large as the original matrix, i.e., perturbation is such that the rank is, at least, not reduced.

Lemma 2 (Rank of Perturbed Hessian). *Under Assumption 4, if $\epsilon < \gamma$ in (2), then $\text{Rank}(\tilde{\mathbf{H}}) \geq \text{Rank}(\mathbf{H})$.*

Proof. First note that from (2), it follows that

$$\lambda_{\min}(\tilde{\mathbf{H}} - \mathbf{H}) \geq -\epsilon, \quad \text{and} \quad \lambda_{\max}(\tilde{\mathbf{H}} - \mathbf{H}) \leq \epsilon.$$

Let $r = \text{Rank}(\mathbf{H})$ and $\tilde{r} = \text{Rank}(\tilde{\mathbf{H}})$. By [4, Theorem 8.4.11], for any $1 \leq j \leq r$, we have

$$\lambda_j(\mathbf{H}) + \lambda_{\min}(\tilde{\mathbf{H}} - \mathbf{H}) \leq \lambda_j(\tilde{\mathbf{H}}) \leq \lambda_j(\mathbf{H}) + \lambda_{\max}(\tilde{\mathbf{H}} - \mathbf{H}),$$

which implies

$$\lambda_j(\mathbf{H}) - \epsilon \leq \lambda_j(\tilde{\mathbf{H}}) \leq \lambda_j(\mathbf{H}) + \epsilon. \quad (22)$$

Now Assumption 4 implies that $|\lambda_j(\mathbf{H})| \geq \gamma$, $1 \leq j \leq r$. Hence, we get

$$\begin{aligned} \lambda_j(\tilde{\mathbf{H}}) &\leq \lambda_j(\mathbf{H}) + \epsilon \leq -\gamma + \epsilon < 0, & \text{if } \lambda_j(\mathbf{H}) < 0, \\ \lambda_j(\tilde{\mathbf{H}}) &\geq \lambda_j(\mathbf{H}) - \epsilon \geq \gamma - \epsilon > 0, & \text{if } \lambda_j(\mathbf{H}) > 0. \end{aligned}$$

Thus, it follows that $\lambda_j(\tilde{\mathbf{H}}) \neq 0, \forall j = 1, \dots, r$, which implies that $\text{Rank}(\tilde{\mathbf{H}}) \geq \text{Rank}(\mathbf{H})$. □

Remark 1. A simple consequence of Lemma 2 is that for strictly-convex objectives, the perturbations remain acute. As a result, for such problems, Algorithm 1 exhibits inherent stability (cf. Definition 1), which resembles, and in fact extends, the results of [51] for the case of the classical Newton's method for strongly convex objectives.

Lemma 2 states that if $\epsilon < \gamma$, the perturbed Hessian is never of lower rank than the original Hessian. In other words, if $\text{Rank}(\tilde{\mathbf{H}}) < \text{Rank}(\mathbf{H})$, then we must necessarily have that $\epsilon \geq \gamma$. From the proof of Lemma 2 and using the fact that $\tilde{\mathbf{H}}$ is symmetric, we have

$$\sigma_i(\tilde{\mathbf{H}}) \geq \gamma - \epsilon, \quad i = 1, \dots, r, \quad (23)$$

where γ is as in Assumption 4. Furthermore, if $\epsilon < \gamma$, we have $r < \tilde{r}$, which by (12) and (22) yields

$$\frac{\epsilon}{C} \leq \sigma_i(\tilde{\mathbf{H}}) \leq \epsilon, \quad i = r + 1, \dots, \tilde{r}. \quad (24)$$

Using Lemma 2, we can establish (15).

Theorem 3. Under Assumptions 4 and 5, and with $\epsilon < \gamma$ in (2), we have (15) with

$$\tilde{\epsilon} \triangleq \frac{4\epsilon}{\gamma} + \sqrt{1-\nu}.$$

Furthermore, in special case of acute perturbation, i.e., $\text{Rank}(\mathbf{H}) = \text{Rank}(\tilde{\mathbf{H}})$, we have

$$\tilde{\epsilon} \triangleq \frac{2\epsilon}{\gamma}.$$

Here, γ and ν are as in Assumptions 4 and 5, respectively.

Proof. By assumption on ϵ , Lemma 2 gives $r \triangleq \text{Rank}(\mathbf{H}) \leq \text{Rank}(\tilde{\mathbf{H}}) \triangleq \tilde{r}$. By (14), (19) and (21b), we will have

$$\begin{aligned} \left\| \mathbf{H}\mathbf{H}^\dagger \mathbf{g} - \tilde{\mathbf{H}}\tilde{\mathbf{H}}^\dagger \mathbf{g} \right\| &= \left\| \mathbf{U}\mathbf{U}^\top \mathbf{g} - \tilde{\mathbf{U}}\tilde{\mathbf{U}}^\top \mathbf{g} \right\| \leq \left\| \mathbf{U}\mathbf{U}^\top \mathbf{g} - \tilde{\mathbf{U}}_1\tilde{\mathbf{U}}_1^\top \mathbf{g} \right\| + \left\| \tilde{\mathbf{U}}_2\tilde{\mathbf{U}}_2^\top \mathbf{g} \right\| \\ &\leq \left\| \mathbf{U}\mathbf{U}^\top \mathbf{g} - \tilde{\mathbf{U}}_1\tilde{\mathbf{U}}_1^\top \mathbf{g} \right\| + \left\| \tilde{\mathbf{U}}_2\tilde{\mathbf{U}}_2^\top \mathbf{g} + \tilde{\mathbf{U}}_\perp\tilde{\mathbf{U}}_\perp^\top \mathbf{g} \right\| \\ &= \left\| \mathbf{U}\mathbf{U}^\top \mathbf{g} - \tilde{\mathbf{U}}_1\tilde{\mathbf{U}}_1^\top \mathbf{g} \right\| \\ &\quad + \left\| \tilde{\mathbf{U}}_2\tilde{\mathbf{U}}_2^\top \mathbf{g} + \tilde{\mathbf{U}}_\perp\tilde{\mathbf{U}}_\perp^\top \mathbf{g} - \mathbf{U}_\perp\mathbf{U}_\perp^\top \mathbf{g} + \mathbf{U}_\perp\mathbf{U}_\perp^\top \mathbf{g} \right\| \\ &= \left\| \mathbf{U}\mathbf{U}^\top \mathbf{g} - \tilde{\mathbf{U}}_1\tilde{\mathbf{U}}_1^\top \mathbf{g} \right\| \\ &\quad + \left\| (\mathbf{I} - \mathbf{U}_\perp\mathbf{U}_\perp^\top) \mathbf{g} - (\mathbf{I} - \tilde{\mathbf{U}}_2\tilde{\mathbf{U}}_2^\top - \tilde{\mathbf{U}}_\perp\tilde{\mathbf{U}}_\perp^\top) \mathbf{g} + \mathbf{U}_\perp\mathbf{U}_\perp^\top \mathbf{g} \right\| \\ &\leq \left\| \mathbf{U}\mathbf{U}^\top \mathbf{g} - \tilde{\mathbf{U}}_1\tilde{\mathbf{U}}_1^\top \mathbf{g} \right\| \\ &\quad + \left\| (\mathbf{I} - \mathbf{U}_\perp\mathbf{U}_\perp^\top) \mathbf{g} - (\mathbf{I} - \tilde{\mathbf{U}}_2\tilde{\mathbf{U}}_2^\top - \tilde{\mathbf{U}}_\perp\tilde{\mathbf{U}}_\perp^\top) \mathbf{g} \right\| \\ &\quad + \left\| \mathbf{U}_\perp\mathbf{U}_\perp^\top \mathbf{g} \right\| \\ &\leq 2 \left\| \mathbf{U}\mathbf{U}^\top \mathbf{g} - \tilde{\mathbf{U}}_1\tilde{\mathbf{U}}_1^\top \mathbf{g} \right\| + \left\| \mathbf{U}_\perp\mathbf{U}_\perp^\top \mathbf{g} \right\| \\ &\leq 4 \left\| \mathbf{H} - \tilde{\mathbf{H}} \right\| \left\| \mathbf{H}^\dagger \right\| \left\| \mathbf{g} \right\| + \sqrt{1-\nu} \left\| \mathbf{g} \right\| \\ &\leq \left(\frac{4\epsilon}{\gamma} + \sqrt{1-\nu} \right) \left\| \mathbf{g} \right\|, \end{aligned}$$

where in the second inequality, we used the Pythagorean theorem as

$$\left\| \tilde{\mathbf{U}}_2\tilde{\mathbf{U}}_2^\top \mathbf{g} + \tilde{\mathbf{U}}_\perp\tilde{\mathbf{U}}_\perp^\top \mathbf{g} \right\|^2 = \left\| \tilde{\mathbf{U}}_2\tilde{\mathbf{U}}_2^\top \mathbf{g} \right\|^2 + \left\| \tilde{\mathbf{U}}_\perp\tilde{\mathbf{U}}_\perp^\top \mathbf{g} \right\|^2 \geq \left\| \tilde{\mathbf{U}}_2\tilde{\mathbf{U}}_2^\top \mathbf{g} \right\|^2,$$

and for the last equality we use the fact that

$$\mathbf{U}\mathbf{U}^\top + \mathbf{U}_\perp\mathbf{U}_\perp^\top = \mathbf{I}, \quad \text{and} \quad \tilde{\mathbf{U}}_1\tilde{\mathbf{U}}_1^\top + \tilde{\mathbf{U}}_2\tilde{\mathbf{U}}_2^\top + \tilde{\mathbf{U}}_\perp\tilde{\mathbf{U}}_\perp^\top = \mathbf{I}.$$

The special case of acute perturbation follows simply from the above without the term involving $\left\| \tilde{\mathbf{U}}_2\tilde{\mathbf{U}}_2^\top \mathbf{g} \right\|$. \square

Theorem 3 also allows us to obtain results similar in spirit to Lemma 1.

Lemma 3. *Under assumptions of Theorem 3, we have*

$$\left\| \tilde{\mathbf{U}}^\top \mathbf{g} \right\|^2 \geq \tilde{\nu} \|\mathbf{g}\|^2, \quad (25a)$$

$$\left\| \tilde{\mathbf{U}}_\perp^\top \mathbf{g} \right\|^2 \leq (1 - \tilde{\nu}) \|\mathbf{g}\|^2, \quad (25b)$$

where

$$\tilde{\nu} \triangleq 2\nu - 1 - \frac{4\epsilon}{\gamma},$$

and $0.5 < \nu \leq 1, \epsilon < \gamma(2\nu - 1)/4$. Furthermore, in special case of acute perturbation, i.e., $\text{Rank}(\mathbf{H}) = \text{Rank}(\tilde{\mathbf{H}})$, we have (25) with

$$\tilde{\nu} \triangleq \nu - \frac{2\epsilon}{\gamma},$$

where $0 < \nu \leq 1, \epsilon < \gamma\nu/2$. Here, γ is as in (18), and $\tilde{\mathbf{U}}, \tilde{\mathbf{U}}_\perp$ are as in (3).

Proof. We have

$$\left\| \tilde{\mathbf{U}}^\top \mathbf{g} \right\|^2 = \mathbf{g}^\top \tilde{\mathbf{U}} \tilde{\mathbf{U}}^\top \mathbf{g} = \mathbf{g}^\top \mathbf{U} \mathbf{U}^\top \mathbf{g} - \mathbf{g}^\top (\mathbf{U} \mathbf{U}^\top - \tilde{\mathbf{U}} \tilde{\mathbf{U}}^\top) \mathbf{g}.$$

Similar to the proof of Theorem 3 and using Lemma 1, we have

$$\begin{aligned} \left| \mathbf{g}^\top \mathbf{U} \mathbf{U}^\top \mathbf{g} - \mathbf{g}^\top \tilde{\mathbf{U}} \tilde{\mathbf{U}}^\top \mathbf{g} \right| &\leq \left| \mathbf{g}^\top \mathbf{U} \mathbf{U}^\top \mathbf{g} - \mathbf{g}^\top \tilde{\mathbf{U}}_1 \tilde{\mathbf{U}}_1^\top \mathbf{g} \right| + \mathbf{g}^\top \tilde{\mathbf{U}}_2 \tilde{\mathbf{U}}_2^\top \mathbf{g} \\ &\leq \frac{2\epsilon}{\gamma} + \mathbf{g}^\top \tilde{\mathbf{U}}_2 \tilde{\mathbf{U}}_2^\top \mathbf{g} \\ &\leq \frac{2\epsilon}{\gamma} + \left| \mathbf{g}^\top \mathbf{U} \mathbf{U}^\top \mathbf{g} - \mathbf{g}^\top \tilde{\mathbf{U}}_1 \tilde{\mathbf{U}}_1^\top \mathbf{g} \right| + \mathbf{g}^\top \mathbf{U}_\perp \mathbf{U}_\perp^\top \mathbf{g} \\ &\leq \left(\frac{4\epsilon}{\gamma} + 1 - \nu \right) \|\mathbf{g}\|^2. \end{aligned}$$

Now, it follows that

$$\left\| \tilde{\mathbf{U}}^\top \mathbf{g} \right\|^2 \geq \mathbf{g}^\top \mathbf{U} \mathbf{U}^\top \mathbf{g} - \left(\frac{4\epsilon}{\gamma} + 1 - \nu \right) \|\mathbf{g}\|^2 \geq \left(2\nu - 1 - \frac{4\epsilon}{\gamma} \right) \|\mathbf{g}\|^2.$$

□

As it is evident from Theorem 3, situations where either $\nu = 1$ or the perturbation is acute, exhibit a certain inherent stability. This observation gives rise to the following definition.

Definition 1 (Inherent Stability). *A perturbation remains inherently stable if one of the following conditions hold:*

- $\tilde{\mathbf{H}}$ is an acute perturbation of \mathbf{H} , i.e., $\text{Rank}(\tilde{\mathbf{H}}) = \text{Rank}(\mathbf{H})$, or
- $\nu = 1$, i.e., $\mathbf{g} \in \text{Range}(\mathbf{H})$, where ν as in Assumption 5.

In light of Definition 1 and Lemma 3, we end this section by specifically stating the perturbation regimes where we develop our stability theory of Section 3.4.

Condition 1. *We consider two perturbation regimes:*

- For general perturbations, we consider (2) with $\epsilon < \gamma(2\nu - 1)/4$ for $0.5 < \nu \leq 1$.
 - For inherently stable perturbations, we consider (2) with $\epsilon < \gamma\nu/2$ for $0 < \nu \leq 1$.
- Here, γ and ν are, respectively, as in Assumptions 4 and 5.

3.4 Convergence Analysis

In this section, we give the convergence analysis of Algorithm 1. For this, in Section 3.4.1 we first consider the case of exact update (5), and subsequently in Section 3.4.2, consider the inexact variant in which the update direction is computed approximately using (6).

3.4.1 Exact Updates

A major ingredient in establishing the convergence of Algorithm 1 using (5) is to obtain an upper-bound on the norm of the exact updates, $\mathbf{p} = -\tilde{\mathbf{H}}^\dagger \mathbf{g}$. This indeed is crucial in light of (12), which implies that $\tilde{\mathbf{H}}^\dagger$ can grow unbounded as $\epsilon \downarrow 0$. However, as in Theorem 3, we can obtain a bound, which fits squarely into the notion of inherently stable perturbations from Definition 1.

Lemma 4 (Stability of Pseudo-inverse of Perturbed Hessian). *Under Assumption 1 as well as Assumptions of Theorem 3, we have*

$$\left\| \tilde{\mathbf{H}}^\dagger \mathbf{g} \right\| \leq \frac{1}{\tilde{\gamma}} \|\mathbf{g}\|,$$

where

$$\tilde{\gamma} \triangleq \left(\frac{1}{\gamma - \epsilon} + C \left(\frac{2}{\gamma} + \frac{\sqrt{1 - \nu}}{\epsilon} \right) \right)^{-1}.$$

Furthermore, in special case of acute perturbation, i.e., $\text{Rank}(\mathbf{H}) = \text{Rank}(\tilde{\mathbf{H}})$, we have

$$\tilde{\gamma} \triangleq \gamma - \epsilon.$$

Here, ϵ, C, γ and ν are, respectively, as in (2), (12), (18) and (20).

Proof. Consider the SVD of $\tilde{\mathbf{H}}^\dagger$ as in (3). Note that (23) implies that $\|\tilde{\Sigma}_1^{-1}\| \leq 1/(\gamma - \epsilon)$. Further, from (24), it follows that $\|\tilde{\Sigma}_2^{-1}\| \leq C/\epsilon$. Now, it follows that

$$\begin{aligned} \|\tilde{\mathbf{H}}^\dagger \mathbf{g}\|^2 &= \left\| \tilde{\mathbf{V}} \begin{bmatrix} \tilde{\Sigma}_1^{-1} & 0 & 0 \\ 0 & \tilde{\Sigma}_2^{-1} & 0 \\ 0 & 0 & 0 \end{bmatrix} \begin{bmatrix} \tilde{\mathbf{U}}_1^\top \\ \tilde{\mathbf{U}}_2^\top \\ \tilde{\mathbf{U}}_\perp^\top \end{bmatrix} \mathbf{g} \right\|^2 \\ &= \left\| \tilde{\Sigma}_1^{-1} \tilde{\mathbf{U}}_1^\top \mathbf{g} \right\|^2 + \left\| \tilde{\Sigma}_2^{-1} \tilde{\mathbf{U}}_2^\top \mathbf{g} \right\|^2 \\ &\leq \frac{1}{(\gamma - \epsilon)^2} \|\mathbf{g}\|^2 + C^2 \left(\frac{2}{\gamma} + \frac{\sqrt{1 - \nu}}{\epsilon} \right)^2 \|\mathbf{g}\|^2, \end{aligned}$$

where the last inequality is obtained using the bound on $\|\tilde{\mathbf{U}}_2^\top \mathbf{g}\| = \|\tilde{\mathbf{U}}_2 \tilde{\mathbf{U}}_2^\top \mathbf{g}\|$ as in the proof of Theorem 3. The result follows from the inequality $\sqrt{a^2 + b^2} \leq a + b$, $\forall a, b \geq 0$. \square

Remark 2. As indicated in Section 3.1, obtaining a bound similar to (19) for $\tilde{\mathbf{H}}$ is entirely dependent on having $\text{Rank}(\mathbf{H}) = \text{Rank}(\tilde{\mathbf{H}})$, which is too stringent to require. Lemma 4 indicates that, when $\text{Rank}(\mathbf{H}) \neq \text{Rank}(\tilde{\mathbf{H}})$, despite the fact that $\|\tilde{\mathbf{H}}^\dagger\|$ can grow unbounded as $\epsilon \downarrow 0$, if $\nu = 1$, we are guaranteed that the action of $\tilde{\mathbf{H}}^\dagger$ on \mathbf{g} , i.e., the exact Newton-MR direction, indeed remains bounded. If $\nu < 1$ and $\text{Rank}(\mathbf{H}) \neq \text{Rank}(\tilde{\mathbf{H}})$, then $\|\tilde{\mathbf{H}}^\dagger \mathbf{g}\|/\|\mathbf{g}\|$ can become increasingly larger with smaller perturbations, resulting in an algorithm that might no longer converge; see the numerical examples of Section 4.1.

For our convergence proofs, we frequently make use of the following result.

Lemma 5 ([48, Lemma 10]). *Consider any $\mathbf{x}, \mathbf{z} \in \mathbb{R}^d$, $0 \leq L < \infty$ and $h : \mathbb{R}^d \rightarrow \mathbb{R}$. If it holds that*

$$\|\nabla h(\mathbf{y}) - \nabla h(\mathbf{x})\| \leq L \|\mathbf{y} - \mathbf{x}\|, \quad \forall \mathbf{y} \in [\mathbf{x}, \mathbf{z}],$$

then, we have

$$h(\mathbf{y}) \leq h(\mathbf{x}) + \langle \nabla h(\mathbf{x}), \mathbf{y} - \mathbf{x} \rangle + \frac{L}{2} \|\mathbf{y} - \mathbf{x}\|^2, \quad \forall \mathbf{y} \in [\mathbf{x}, \mathbf{z}].$$

If we take $h(\mathbf{x}) = \|\mathbf{g}(\mathbf{x})\|^2/2$, the constant L in Lemma 5 is $L(\mathbf{x}_0)$ in Assumption 3.

Theorem 4 (Global Convergence of Algorithm 1 With Exact Updates). *Under Assumptions 1 to 5 and Condition 1, for the iterates of Algorithm 1 with exact updates (5), we have*

$$\|\mathbf{g}_{k+1}\|^2 \leq \left(1 - \frac{4\rho\tilde{\nu}\tilde{\gamma}^2}{L(\mathbf{x}_0)} \left((1-\rho)\tilde{\nu} - \frac{\epsilon}{\tilde{\gamma}}\right)\right) \|\mathbf{g}_k\|^2,$$

where $\rho, L(\mathbf{x}_0), \tilde{\nu}$ and $\tilde{\gamma}$ are, respectively, as in (7), Assumption 3, and Lemmas 3 and 4.

Proof. From Lemma 5 with $\mathbf{x} = \mathbf{x}_k$, $\mathbf{z} = \mathbf{x}_k + \mathbf{p}_k$, $\mathbf{y} = \mathbf{x}_k + \alpha\mathbf{p}_k$, and $h(\mathbf{x}) = \|\mathbf{g}(\mathbf{x})\|^2/2$, we have

$$\|\mathbf{g}_{k+1}\|^2 \leq \|\mathbf{g}_k\|^2 + 2\alpha \langle \mathbf{p}_k, \mathbf{H}_k \mathbf{g}_k \rangle + \alpha^2 L(\mathbf{x}_0) \|\mathbf{p}_k\|^2 \quad (26)$$

Now to obtain a sufficient condition on α to satisfy (7), we consider the inequality

$$2\alpha \langle \mathbf{p}_k, \mathbf{H}_k \mathbf{g}_k \rangle + \alpha^2 L(\mathbf{x}_0) \|\mathbf{p}_k\|^2 \leq 2\rho\alpha \langle \mathbf{p}_k, \tilde{\mathbf{H}}_k \mathbf{g}_k \rangle,$$

we used (26) as upper bound on $\|\mathbf{g}_{k+1}\|^2$. Rearranging gives

$$\alpha \leq \frac{2 \left(\rho \langle \mathbf{g}_k, \tilde{\mathbf{H}}_k \mathbf{p}_k \rangle - \langle \mathbf{g}_k, \mathbf{H}_k \mathbf{p}_k \rangle \right)}{L(\mathbf{x}_0) \|\mathbf{p}_k\|^2}. \quad (27)$$

By (2) and Lemmas 3 and 4, we have

$$\begin{aligned} \rho \langle \mathbf{g}_k, \tilde{\mathbf{H}}_k \mathbf{p}_k \rangle - \langle \mathbf{g}_k, \mathbf{H}_k \mathbf{p}_k \rangle &= -(1-\rho) \langle \mathbf{g}_k, \tilde{\mathbf{H}}_k \mathbf{p}_k \rangle - \langle \mathbf{g}_k, (\mathbf{H}_k - \tilde{\mathbf{H}}_k) \mathbf{p}_k \rangle \\ &\geq (1-\rho)\tilde{\nu} \|\mathbf{g}_k\|^2 - \frac{\epsilon}{\tilde{\gamma}} \|\mathbf{g}_k\|^2, \end{aligned}$$

which in turn gives

$$\alpha \leq \frac{2\tilde{\gamma}^2}{L(\mathbf{x}_0)} \left((1-\rho)\tilde{\nu} - \frac{\epsilon}{\tilde{\gamma}} \right).$$

In other words, the lower bound on the step-size returned by line search is $\alpha_k \geq \alpha$. From (7) with this α , we have

$$\begin{aligned} \|\mathbf{g}_{k+1}\|^2 &\leq \|\mathbf{g}_k\|^2 + 2\rho\alpha_k \langle \tilde{\mathbf{H}}_k \mathbf{p}_k, \mathbf{g}_k \rangle \\ &\leq \|\mathbf{g}_k\|^2 - 2\rho\alpha_k \tilde{\nu} \|\mathbf{g}_k\|^2 \\ &\leq \left(1 - \frac{4\rho\tilde{\nu}\tilde{\gamma}^2}{L(\mathbf{x}_0)} \left((1-\rho)\tilde{\nu} - \frac{\epsilon}{\tilde{\gamma}}\right)\right) \|\mathbf{g}_k\|^2. \end{aligned}$$

□

In particular, for inherently stable perturbations from Definition 1, we have the following convergence guarantee.

Corollary 1 (Global Convergence of Algorithm 1 With Exact Updates Under Inherent Stability). *Under the assumptions of Theorem 4, for inherently stable perturbations, we have*

$$\|\mathbf{g}_{k+1}\|^2 \leq (1 - \eta) \|\mathbf{g}_k\|^2,$$

where

- if the perturbation is acute, then

$$\eta \triangleq \frac{4\rho(\nu\gamma - 2\epsilon)(\gamma - \epsilon)^2}{\gamma^2 L(\mathbf{x}_0)} \left((1 - \rho)(\nu\gamma - 2\epsilon) - \frac{\gamma\epsilon}{\gamma - \epsilon} \right),$$

- otherwise if $\nu = 1$ then

$$\eta \triangleq \frac{4\rho(\gamma - 4\epsilon)(\gamma - \epsilon)^2}{((1 + 2C)\gamma - 2C\epsilon)^2 L(\mathbf{x}_0)} \left((1 - \rho)(\gamma - 4\epsilon) - \frac{((1 + 2C)\gamma - 2C\epsilon)\epsilon}{\gamma - \epsilon} \right).$$

Here, $\rho, C, L(\mathbf{x}_0)$ and γ are as in (7), (12), (17) and (18), respectively.

Remark 3. For acute perturbations, we see from Corollary 1 that the convergence rate in the limit where $\epsilon \downarrow 0$, matches that of unperturbed algorithm in [48]. For the case where $\nu = 1$ but the perturbation is not acute, the limiting rate is worse than the unperturbed algorithm, and we believe that this is simply a byproduct of our analysis here.

Remark 4. Corollary 1 shows that for perturbations that are inherently stable as defined in Definition 1, Algorithm 1 with exact update (5) remains stable as $\epsilon \downarrow 0$ and is guaranteed to converge for small enough ϵ . For general perturbations, since we have

$$\begin{aligned} \langle \mathbf{H}\mathbf{g}, \mathbf{p} \rangle &= -\langle \mathbf{H}\mathbf{g}, \tilde{\mathbf{H}}^\dagger \mathbf{g} \rangle = -\langle (\mathbf{H} - \tilde{\mathbf{H}} + \tilde{\mathbf{H}}) \mathbf{g}, \tilde{\mathbf{H}}^\dagger \mathbf{g} \rangle \\ &= -\langle (\mathbf{H} - \tilde{\mathbf{H}}) \mathbf{g}, \tilde{\mathbf{H}}^\dagger \mathbf{g} \rangle - \langle \tilde{\mathbf{H}}\mathbf{g}, \tilde{\mathbf{H}}^\dagger \mathbf{g} \rangle \leq \left(\frac{\epsilon}{\tilde{\gamma}} - \tilde{\nu} \right) \|\mathbf{g}\|^2, \end{aligned}$$

a bit of algebraic computations reveal that to guarantee descent it is sufficient to have

$$\epsilon < \frac{\gamma \left(2a + b + 1 - \sqrt{(2a + b + 1)^2 - 8ab} \right)}{4a},$$

where

$$\begin{aligned} a &\triangleq C + 2, \\ b &\triangleq 2\nu - 1 - C\sqrt{1 - \nu}. \end{aligned}$$

As a result, if $b > 0$, i.e.,

$$\nu > \delta(C), \text{ where } \delta(C) \triangleq \frac{\sqrt{(C^2 + 4)^2 - 16} - (C^2 - 4)}{8} < 1, \forall C \geq 1,$$

Algorithm 1 remains stable as $\epsilon \downarrow 0$ and we can still guarantee descent for small enough ϵ . Otherwise, as $\epsilon \downarrow 0$, the search direction, \mathbf{p} , might no longer be a descent direction and the steps-size from the line-search will shrink to zero; see the numerical examples of Section 4.1.

Theorem 5 (Error Recursion of Algorithm 1 With $\alpha_k = 1$ and Exact Updates). *Under the assumptions of Theorem 4 with Assumption 3 replaced with (16b), for the iterates of Algorithm 1 with $\alpha_k = 1$ and exact update, we have*

$$\|\mathbf{g}(\mathbf{x}_{k+1})\| \leq \frac{L_{\mathbf{H}}}{2\tilde{\gamma}^2} \|\mathbf{g}(\mathbf{x}_k)\|^2 + \left(\frac{\epsilon}{\tilde{\gamma}} + \sqrt{1 - \tilde{\nu}} \right) \|\mathbf{g}(\mathbf{x}_k)\|.$$

where $L_{\mathbf{H}}, \tilde{\nu}$ and $\tilde{\gamma}$ are, respectively, as in (16b) and Lemmas 3 and 4.

Proof. With $\alpha_k = 1$, we can apply Lemma 3 and the mean-value theorem [21] for vector-valued functions to get

$$\begin{aligned} \|\mathbf{g}(\mathbf{x}_{k+1})\| &= \|\mathbf{g}(\mathbf{x}_k + \mathbf{p}_k)\| \\ &= \left\| \mathbf{g}(\mathbf{x}_k) + \int_0^1 \mathbf{H}(\mathbf{x}_k + t\mathbf{p}_k) \mathbf{p}_k dt \right\| \\ &= \left\| \left(\tilde{\mathbf{U}}\tilde{\mathbf{U}}^\top + \tilde{\mathbf{U}}_\perp\tilde{\mathbf{U}}_\perp^\top \right) \mathbf{g}(\mathbf{x}_k) + \int_0^1 \mathbf{H}(\mathbf{x}_k + t\mathbf{p}_k) \mathbf{p}_k dt \right\| \\ &\leq \left\| \tilde{\mathbf{H}}(\mathbf{x}_k)\tilde{\mathbf{H}}^\dagger(\mathbf{x}_k)\mathbf{g}(\mathbf{x}_k) + \int_0^1 \mathbf{H}(\mathbf{x}_k + t\mathbf{p}_k) \mathbf{p}_k dt \right\| + \left\| \tilde{\mathbf{U}}_\perp\tilde{\mathbf{U}}_\perp^\top\mathbf{g}(\mathbf{x}_k) \right\| \\ &\leq \frac{1}{\tilde{\gamma}} \|\mathbf{g}(\mathbf{x}_k)\| \int_0^1 \left\| \mathbf{H}(\mathbf{x}_k + t\mathbf{p}_k) - \tilde{\mathbf{H}}(\mathbf{x}_k) \right\| dt + \sqrt{1 - \tilde{\nu}} \|\mathbf{g}(\mathbf{x}_k)\| \\ &\leq \frac{1}{\tilde{\gamma}} \|\mathbf{g}(\mathbf{x}_k)\| \int_0^1 \|\mathbf{H}(\mathbf{x}_k + t\mathbf{p}_k) - \mathbf{H}(\mathbf{x}_k)\| dt + \frac{\epsilon}{\tilde{\gamma}} \|\mathbf{g}(\mathbf{x}_k)\| + \sqrt{1 - \tilde{\nu}} \|\mathbf{g}(\mathbf{x}_k)\| \\ &\leq \frac{L_{\mathbf{H}}}{2\tilde{\gamma}^2} \|\mathbf{g}(\mathbf{x}_k)\|^2 + \left(\frac{\epsilon}{\tilde{\gamma}} + \sqrt{1 - \tilde{\nu}} \right) \|\mathbf{g}(\mathbf{x}_k)\| \end{aligned}$$

□

Corollary 2 (Error Recursion of Algorithm 1 With $\alpha_k = 1$ and Exact Updates Under Inherent Stability). *Under the assumptions of Theorem 5, for inherently stable perturbations, we have*

$$\|\mathbf{g}(\mathbf{x}_{k+1})\| \leq c_1 \|\mathbf{g}(\mathbf{x}_k)\|^2 + c_2 \|\mathbf{g}(\mathbf{x}_k)\|,$$

where where

- if the perturbation is acute, then

$$c_1 = \frac{L_{\mathbf{H}}}{2(\gamma - \epsilon)^2}, \quad c_2 = \frac{\epsilon}{(\gamma - \epsilon)} + \sqrt{1 - \left(\nu - \frac{2\epsilon}{\gamma}\right)},$$

- otherwise if $\nu = 1$ then

$$c_1 = \frac{((1 + 2C)\gamma - 2C\epsilon)^2 L_{\mathbf{H}}}{2\gamma^2 (\gamma - \epsilon)^2}, \quad c_2 = \frac{((1 + 2C)\gamma - 2C\epsilon)\epsilon}{\gamma(\gamma - \epsilon)} + 2\sqrt{\frac{\epsilon}{\gamma}},$$

Here, C , $L_{\mathbf{H}}$, γ and ν are as in (12), (16b), (19) and (20), respectively.

Remark 5. Corollary 2 shows that, under inherent stability and for small ϵ , we obtain a problem-independent local linear convergence rate. For example, consider any ϵ small enough for which we get $c_2 < 1$. Then for any $c_2 < c < 1$, there exists a $r > 0$ for which if $\|\mathbf{g}_k\| \leq r$, we have $\|\mathbf{g}_{k+1}\| \leq c \|\mathbf{g}_k\|$. In the absence of inherent stability, again, Algorithm 1 might in fact stagnate as the step-size can shrink to zero (cf. Remark 4).

3.4.2 Inexact Updates

We now turn to convergence analysis of Newton-MR using inexact update (6). Clearly, the inexactness tolerance θ has to be chosen with regard to Lemma 3. Indeed, suppose the conditions of Lemma 3 is satisfied. With exact solution to (5), we have

$$\left\langle \mathbf{g}_k, \tilde{\mathbf{H}}_k \mathbf{p}_k + \mathbf{g}_k \right\rangle = - \left\langle \mathbf{g}_k, \tilde{\mathbf{H}}_k \left[\tilde{\mathbf{H}}_k \right]^\dagger \mathbf{g}_k \right\rangle + \|\mathbf{g}_k\|^2 \leq (1 - \tilde{\nu}) \|\mathbf{g}_k\|^2,$$

where $\tilde{\nu}$ is defined in Lemma 3. This in turn implies that it is sufficient to chose θ such that $\theta \leq 1 - \tilde{\nu}$, giving rise to the following condition in inexactness tolerance.

Condition 2 (Inexactness Tolerance). *The inexactness tolerance, θ , in (6) is chosen such that $1 - \tilde{\nu} \leq \theta < 1$, $\tilde{\nu}$ is defined in Lemma 3.*

As advocated in [48], due to several desirable advantages, MINRES-QLP [19] is the method of choice for inexact variant of Newton-MR in which the search direction is

computed from (6). Recall that, at the k^{th} iteration of Algorithm 1, the t^{th} iteration of MINRES-QLP can be represented as

$$\mathbf{p}_k^{(t)} = \arg \min \|\mathbf{p}\|^2 \quad \text{s.t.} \quad \mathbf{p} \in \underset{\hat{\mathbf{p}} \in \mathcal{K}_t}{\text{Arg min}} \left\| \tilde{\mathbf{H}}_k \hat{\mathbf{p}} + \mathbf{g}_k \right\|^2, \quad (28)$$

where $\mathcal{K}_t = \mathcal{K}_t(\tilde{\mathbf{H}}_k, \mathbf{g}_k)$ or $\mathcal{K}_t = \mathcal{K}_t(\tilde{\mathbf{H}}_k, \tilde{\mathbf{H}}_k \mathbf{g}_k)$.

Before delving deeper into the analysis of this section, we first give some simple properties of solutions to (6) obtained from MINRES-QLP.

Lemma 6. *For any solution to (6) obtained from MINRES-QLP, we have*

$$\left\| \tilde{\mathbf{H}}_k \mathbf{p}_k \right\| \leq \|\mathbf{g}_k\|, \quad (29a)$$

$$\left\| \tilde{\mathbf{H}}_k \mathbf{p}_k + \mathbf{g}_k \right\| \leq \sqrt{2\theta} \|\mathbf{g}_k\|. \quad (29b)$$

Proof. It has been shown in [19, Lemma 3.3 and Section 6.6] that for $\mathbf{p}_k^{(t)}$ as in (28), $\left\| \tilde{\mathbf{H}}_k \mathbf{p}_k^{(t)} \right\|$ is monotonically non-decreasing with t . As a result, we obtain

$$\left\| \tilde{\mathbf{H}}_k \mathbf{p}_k \right\| \leq \left\| \tilde{\mathbf{H}}_k \left[\tilde{\mathbf{H}}_k \right]^\dagger \mathbf{g}_k \right\| = \left\| \tilde{\mathbf{U}} \tilde{\mathbf{U}}^\top \mathbf{g}_k \right\| \leq \|\mathbf{g}_k\|.$$

From (29a), we can get

$$\begin{aligned} \left\| \tilde{\mathbf{H}}_k \mathbf{p}_k + \mathbf{g}_k \right\|^2 &= \left\| \tilde{\mathbf{H}}_k \mathbf{p}_k \right\|^2 + \|\mathbf{g}_k\|^2 + 2 \left\langle \tilde{\mathbf{H}}_k \mathbf{p}_k, \mathbf{g}_k \right\rangle \\ &\leq 2 \|\mathbf{g}_k\|^2 - 2(1 - \theta) \|\mathbf{g}_k\|^2 = 2\theta \|\mathbf{g}_k\|^2. \end{aligned}$$

□

Here, as in Section 3.4.1, establishing the convergence of Algorithm 1 using (6) hinges upon obtaining a bound similar to that in Lemma 4, but in terms of \mathbf{p}_k from (6). A naïve application of (12) and (29a) gives

$$\|\mathbf{p}_k\| \leq \frac{C}{\epsilon} \left\| \tilde{\mathbf{H}}_k \mathbf{p}_k \right\| \leq \frac{C}{\epsilon} \|\mathbf{g}_k\|,$$

which implies the search direction can become unbounded as $\epsilon \downarrow 0$. Unfortunately, the norms of the iterates of MINRES-QLP are not necessarily monotonic; see [12, 19, 20, 28]. As a result, although by Lemma 4, we have an upper bound on the final iterate, i.e., the exact solution (4), the intermediate iterates from (28) may have larger norms. Nonetheless, as part of the results of this section, we show that indeed all iterates of MINRES-QLP from (28) are bounded in the same way as in Lemma 4, which can be of independent interest; see Lemma 9.

To achieve this, we first show that (28) can be decoupled into two separate constrained least squares problems. We then show that the solution to each of these least squares problems is indeed bounded.

Lemma 7. For any symmetric matrix $\mathbf{A} \in \mathbb{R}^{d \times d}$ and $\mathbf{b} \in \mathbb{R}^d$, consider the problem

$$\mathbf{x}^* = \arg \min \|\mathbf{x}\|^2 \quad \text{s.t.} \quad \mathbf{x} \in \underset{\hat{\mathbf{x}} \in \mathcal{K}_t}{\text{Arg min}} \|\mathbf{A}\hat{\mathbf{x}} - \mathbf{b}\|^2, \quad (30)$$

where \mathcal{K}_t is any Krylov subspace. Let \mathbf{P}_1 and \mathbf{P}_2 be orthogonal projectors onto \mathbf{A} -invariant sub-spaces. Further, assume that $\mathbf{P}_1\mathbf{P}_2 = \mathbf{P}_2\mathbf{P}_1 = \mathbf{0}$ and $\text{Range}(\mathbf{A}) = \text{Range}(\mathbf{P}_1) \oplus \text{Range}(\mathbf{P}_2)$, where \oplus denotes the direct sum. We have

$$\mathbf{x}^* = \arg \min_{\mathbf{x}_1 \in \mathbf{P}_1 \cdot \mathcal{K}_t} \|\mathbf{A}\mathbf{x}_1 - \mathbf{P}_1\mathbf{b}\|^2 + \arg \min_{\mathbf{x}_2 \in \mathbf{P}_2 \cdot \mathcal{K}_t} \|\mathbf{A}\mathbf{x}_2 - \mathbf{P}_2\mathbf{b}\|^2. \quad (31)$$

Proof. First note that since \mathbf{A} is symmetric and $\mathbf{P}_i, i = 1, 2$, are the orthogonal projectors onto invariant sub-spaces of \mathbf{A} , we have $\mathbf{P}_i\mathbf{A} = \mathbf{A}\mathbf{P}_i, i = 1, 2$. Let $\mathbf{P} = \mathbf{P}_1 + \mathbf{P}_2$. By Pythagoras theorem we have

$$\|\mathbf{A}\mathbf{x} - \mathbf{b}\|^2 = \|\mathbf{P}\mathbf{A}\mathbf{x} - \mathbf{P}\mathbf{b}\|^2 + \|(\mathbf{I} - \mathbf{P})\mathbf{b}\|^2.$$

Noting that $\mathbf{x}^* \in \text{Range}(\mathbf{A})$ (see [48, Lemma 7]), we can rewrite (30) as

$$\mathbf{x}^* = \arg \min_{\mathbf{x} \in \mathbf{P} \cdot \mathcal{K}_t} \|\mathbf{A}\mathbf{P}\mathbf{x} - \mathbf{P}\mathbf{b}\|^2.$$

Defining $\mathbf{x}_i = \mathbf{P}_i\mathbf{x}, i = 1, 2$, for any $\mathbf{x} \in \text{Range}(\mathbf{A})$, we can write $\mathbf{x} = \mathbf{x}_1 + \mathbf{x}_2$. Noting that \mathbf{P}_1 and \mathbf{P}_2 are orthogonal projections onto orthogonal sub-spaces, we have

$$\begin{aligned} \mathbf{x}^* &= \arg \min_{\substack{\mathbf{x}_1 \in \mathbf{P}_1 \cdot \mathcal{K}_t \\ \mathbf{x}_2 \in \mathbf{P}_2 \cdot \mathcal{K}_t}} \|\mathbf{A}(\mathbf{P}_1\mathbf{x}_1 + \mathbf{P}_2\mathbf{x}_2) - (\mathbf{P}_1 + \mathbf{P}_2)\mathbf{b}\|^2 \\ &= \arg \min_{\substack{\mathbf{x}_1 \in \mathbf{P}_1 \cdot \mathcal{K}_t \\ \mathbf{x}_2 \in \mathbf{P}_2 \cdot \mathcal{K}_t}} \|\mathbf{P}_1\mathbf{A}\mathbf{x}_1 + \mathbf{P}_2\mathbf{A}\mathbf{x}_2 - (\mathbf{P}_1 + \mathbf{P}_2)\mathbf{b}\|^2 \\ &= \arg \min_{\substack{\mathbf{x}_1 \in \mathbf{P}_1 \cdot \mathcal{K}_t \\ \mathbf{x}_2 \in \mathbf{P}_2 \cdot \mathcal{K}_t}} \left(\|\mathbf{P}_1\mathbf{A}\mathbf{x}_1 - \mathbf{P}_1\mathbf{b}\|^2 + \|\mathbf{P}_2\mathbf{A}\mathbf{x}_2 - \mathbf{P}_2\mathbf{b}\|^2 \right) \\ &= \arg \min_{\mathbf{x}_1 \in \mathbf{P}_1 \cdot \mathcal{K}_t} \|\mathbf{A}\mathbf{x}_1 - \mathbf{P}_1\mathbf{b}\|^2 + \arg \min_{\mathbf{x}_2 \in \mathbf{P}_2 \cdot \mathcal{K}_t} \|\mathbf{A}\mathbf{x}_2 - \mathbf{P}_2\mathbf{b}\|^2. \end{aligned}$$

□

The following lemma gives a bound on the solution of each of decoupled terms in (31).

Lemma 8. For any symmetric matrix $\mathbf{A} \in \mathbb{R}^{d \times d}$ and $\mathbf{b} \in \mathbb{R}^d$, consider the problem

$$\mathbf{x}^* \triangleq \arg \min_{\mathbf{x} \in \mathbf{P} \cdot \mathcal{K}_t} \|\mathbf{A}\mathbf{x} - \mathbf{P}\mathbf{b}\|, \quad (32)$$

where \mathbf{P} is the orthogonal projector onto a \mathbf{A} -invariant subspace and \mathcal{K}_t is $\mathcal{K}_t(\mathbf{A}, \mathbf{b})$

or $\mathcal{K}_t(\mathbf{A}, \mathbf{Ab})$, for $t \in \{1, 2, \dots, \text{Rank}(\mathbf{AP})\}$. We have

$$\|\mathbf{x}^*\| \leq \|\mathbf{Pb}\| \left\| [\mathbf{AP}]^\dagger \right\|.$$

Proof. Clearly, we can replace (32) with an equivalent formulation as

$$\mathbf{x}^* = \arg \min_{\mathbf{x} \in \mathbf{P} \cdot \mathcal{K}_t} \|\mathbf{APx} - \mathbf{Pb}\|.$$

We prove the result for when $\mathcal{K}_t = \mathcal{K}_t(\mathbf{A}, \mathbf{b})$ as the case of $\mathcal{K}_t = \mathcal{K}_t(\mathbf{A}, \mathbf{Ab})$ is proven similarly. As before, since \mathbf{A} is symmetric and \mathbf{P} is the orthogonal projector onto an invariant sub-spaces of \mathbf{A} , we have $\mathbf{PA} = \mathbf{AP}$, hence \mathbf{AP} is also symmetric. Consider applying Lanczos process to obtain the decomposition

$$\mathbf{APQ}_t = \mathbf{Q}_{t+1}\mathbf{T}_t,$$

where $\mathbf{T}_t \in \mathbb{R}^{(t+1) \times t}$ and $\mathbf{Q}_t = [\mathbf{q}_1, \mathbf{q}_2, \dots, \mathbf{q}_t]$ is an orthonormal basis for the Krylov subspace $\mathbf{P} \cdot \mathcal{K}_t = \mathcal{K}_t(\mathbf{AP}, \mathbf{Pb})$ and $\mathbf{Q}_{t+1} = [\mathbf{Q}_t \mid \mathbf{q}_{t+1}]$ with $\mathbf{Q}_t^\top \mathbf{q}_{t+1} = \mathbf{0}$. Recall that one can find $\mathbf{x}^* = \mathbf{Q}_t \mathbf{y}^*$ where

$$\mathbf{y}^* \triangleq \arg \min_{\mathbf{y} \in \mathbb{R}^t} \|\mathbf{T}_t \mathbf{y} - [\mathbf{Q}_{t+1}]^\top \mathbf{Pb}\|.$$

It follows that

$$\|\mathbf{x}^*\| = \|\mathbf{Q}_t \mathbf{y}^*\| = \|\mathbf{y}^*\| = \left\| [\mathbf{T}_t]^\dagger [\mathbf{Q}_{t+1}]^\top \mathbf{Pb} \right\|.$$

Also, we have

$$\begin{aligned} \left\| [\mathbf{T}_t]^\dagger \right\| &= \left\| [\mathbf{Q}_{t+1} \mathbf{T}_t [\mathbf{Q}_t]^\top]^\dagger \right\| \\ &\leq \left\| [\mathbf{Q}_{t+2} \mathbf{T}_{t+1} [\mathbf{Q}_{t+1}]^\top]^\dagger \right\| \leq \dots \leq \left\| [\mathbf{AP}]^\dagger \right\|, \end{aligned}$$

where the first equality is obtained by noting that

$$[\mathbf{Q}_{t+1} \mathbf{T}_t [\mathbf{Q}_t]^\top]^\dagger = [\mathbf{T}_t [\mathbf{Q}_t]^\top]^\dagger [\mathbf{Q}_{t+1}]^\top = \mathbf{Q}_t \mathbf{T}_t^\dagger [\mathbf{Q}_{t+1}]^\top,$$

and the series of inequalities follow from the result in [11]. So, we finally get

$$\|\mathbf{x}^*\| = \left\| [\mathbf{T}_t]^\dagger [\mathbf{Q}_{t+1}]^\top \mathbf{Pb} \right\| \leq \|\mathbf{Pb}\| \left\| [\mathbf{T}_t]^\dagger \right\| \leq \|\mathbf{Pb}\| \left\| [\mathbf{AP}]^\dagger \right\|.$$

□

We are now ready to prove a result similar to Lemma 4 for the case of inexact updates.

Lemma 9. Under Assumptions of Lemma 4, for the iterates of MINRES-QLP in (28), we have

$$\left\| \mathbf{p}_k^{(t)} \right\| \leq \frac{1}{\tilde{\gamma}} \|\mathbf{g}_k\|, \quad t = 1, 2, \dots, \text{Rank}(\tilde{\mathbf{H}}_k),$$

where $\tilde{\gamma}$ is as in Lemma 4.

Proof. For simplicity, we drop the dependence on k and t . Let $\tilde{\mathbf{P}}_1, \tilde{\mathbf{P}}_2$ and $\tilde{\mathbf{P}}_\perp$ denote the projectors $\tilde{\mathbf{U}}_1 \tilde{\mathbf{U}}_1^\top, \tilde{\mathbf{U}}_2 \tilde{\mathbf{U}}_2^\top$ and $\tilde{\mathbf{U}}_\perp \tilde{\mathbf{U}}_\perp^\top$, respectively, where $\tilde{\mathbf{U}}_1, \tilde{\mathbf{U}}_2$ and $\tilde{\mathbf{U}}_\perp$ are defined in (3). Also, let $\tilde{\mathbf{P}} = \tilde{\mathbf{P}}_1 + \tilde{\mathbf{P}}_2$. Using Lemma 7, we can write (28) as $\mathbf{p} = \mathbf{p}_1 + \mathbf{p}_2$, where

$$\begin{aligned} \mathbf{p}_1 &= \arg \min_{\mathbf{p} \in \tilde{\mathbf{P}}_1 \cdot \mathcal{K}_t} \left\| \tilde{\mathbf{H}}\mathbf{p} + \tilde{\mathbf{P}}_1 \mathbf{g} \right\|, \\ \mathbf{p}_2 &= \arg \min_{\mathbf{p} \in \tilde{\mathbf{P}}_2 \cdot \mathcal{K}_t} \left\| \tilde{\mathbf{H}}\mathbf{p} + \tilde{\mathbf{P}}_2 \mathbf{g} \right\|. \end{aligned}$$

From Lemma 8 and (23), it follows that

$$\|\mathbf{p}_1\| \leq \left\| \tilde{\mathbf{P}}_1 \mathbf{g} \right\| \left\| \left[\tilde{\mathbf{H}} \tilde{\mathbf{P}}_1 \right]^\dagger \right\| = \left\| \tilde{\mathbf{U}}_1 \tilde{\mathbf{U}}_1^\top \mathbf{g} \right\| \left\| \left[\tilde{\mathbf{U}}_1 \tilde{\mathbf{U}}_1^\top \tilde{\mathbf{H}} \right]^\dagger \right\| \leq \frac{1}{\gamma - \epsilon} \|\mathbf{g}\|.$$

Similarly, by (21b) and (24), Theorem 2, and Lemma 8, we have

$$\begin{aligned} \|\mathbf{p}_2\| &\leq \left\| \tilde{\mathbf{P}}_2 \mathbf{g} \right\| \left\| \left[\tilde{\mathbf{H}} \tilde{\mathbf{P}}_2 \right]^\dagger \right\| \\ &\leq \left\| \left(\tilde{\mathbf{U}}_2 \tilde{\mathbf{U}}_2^\top + \tilde{\mathbf{U}}_\perp \tilde{\mathbf{U}}_\perp^\top \right) \mathbf{g} \right\| \left\| \left[\tilde{\mathbf{U}}_2 \tilde{\mathbf{U}}_2^\top \tilde{\mathbf{H}} \right]^\dagger \right\| \\ &\leq \left\| \left(\tilde{\mathbf{U}}_2 \tilde{\mathbf{U}}_2^\top + \tilde{\mathbf{U}}_\perp \tilde{\mathbf{U}}_\perp^\top - \mathbf{U}_\perp \mathbf{U}_\perp^\top + \mathbf{U}_\perp \mathbf{U}_\perp^\top \right) \mathbf{g} \right\| \left\| \left[\tilde{\mathbf{U}}_2 \tilde{\mathbf{U}}_2^\top \tilde{\mathbf{H}} \right]^\dagger \right\| \\ &\leq \frac{C}{\epsilon} \left\| \left(\tilde{\mathbf{U}}_1 \tilde{\mathbf{U}}_1^\top - \mathbf{U} \mathbf{U}^\top + \mathbf{U}_\perp \mathbf{U}_\perp^\top \right) \mathbf{g} \right\| \\ &\leq \frac{C}{\epsilon} \left(\frac{2\epsilon}{\gamma} + \sqrt{1 - \nu} \right) \|\mathbf{g}\|, \end{aligned}$$

which gives us

$$\|\mathbf{p}_2\| \leq C \left(\frac{2}{\gamma} + \frac{\sqrt{1 - \nu}}{\epsilon} \right) \|\mathbf{g}\|.$$

Finally, we obtain

$$\|\mathbf{p}\|^2 = \|\mathbf{p}_1 + \mathbf{p}_2\|^2 = \|\mathbf{p}_1\|^2 + \|\mathbf{p}_2\|^2 \leq \left(\left(\frac{1}{\gamma - \epsilon} \right)^2 + \left(C \left(\frac{2}{\gamma} + \frac{\sqrt{1 - \nu}}{\epsilon} \right) \right)^2 \right) \|\mathbf{g}\|^2.$$

The result follows from the inequality $\sqrt{a^2 + b^2} \leq a + b, \forall a, b \geq 0$. \square

The inexactness condition in (6) involves two criteria for an approximate solution \mathbf{p}_k , namely feasibility of \mathbf{p}_k in (6) and that $\mathbf{p}_k \in \text{Range}(\tilde{\mathbf{H}}_k)$. When $\mathbf{g}_k \in \text{Range}(\tilde{\mathbf{H}}_k)$, the latter is enforced naturally as a result of MINRES-QLP's underlying Krylov subspace. However, in cases where $\mathbf{g}_k \notin \text{Range}(\tilde{\mathbf{H}}_k)$, one could simply modify the Krylov subspace as described in [48]. To allow for unification of the results of this section, we define *range-invariant* Krylov subspace, which encapsulate these variants.

Definition 2 (Range-invariant Krylov Subspace). *For any symmetric matrix \mathbf{A} , the range-invariant Krylov subspace is defined as follows.*

(i) *If $\mathbf{b} \in \text{Range}(\mathbf{A})$, we can consider the usual $\mathcal{K}_t(\mathbf{A}, \mathbf{b})$, e.g., MINRES [46].*

(ii) *Otherwise, we can always employ $\mathcal{K}_t(\mathbf{A}, \mathbf{A}\mathbf{b})$, e.g., MR-II [32].*

Here, $t = 1, \dots, \text{Rank}(\mathbf{A})$.

In the subsequent discussion, we always assume that MINRES-QLP used within Algorithm 1 generates iterates from an appropriate range-invariant Krylov subspace, $\mathcal{K}_t(\tilde{\mathbf{H}}_k, \mathbf{g}_k)$ or $\mathcal{K}_t(\tilde{\mathbf{H}}_k, \tilde{\mathbf{H}}_k \mathbf{g}_k)$ (cf. (28)).

Now, similar with the proofs for exact updates Theorem 4, we can obtain the following results for Algorithm 1 with inexact updates satisfying (6).

Theorem 6 (Global Convergence of Algorithm 1 With Inexact Updates). *Under Assumptions 1 to 5 and Conditions 1 and 2, for the iterates of Algorithm 1 with inexact updates, we have*

$$\|\mathbf{g}_{k+1}\|^2 \leq \left(1 - \frac{4\rho\tilde{\gamma}^2(1-\theta)}{L(\mathbf{x}_0)} \left((1-\rho)(1-\theta) - \frac{\epsilon}{\tilde{\gamma}} \right)\right) \|\mathbf{g}_k\|^2$$

where $\rho, L(\mathbf{x}_0), \tilde{\nu}, \tilde{\gamma}$ and θ are, respectively, as in (7), Assumption 3, Lemmas 3 and 4, and Condition 2.

Proof. Similar with the proof for Theorem 4, by (2) and (6) and Lemma 9, we have

$$\begin{aligned} \rho \langle \mathbf{g}_k, \tilde{\mathbf{H}}_k \mathbf{p}_k \rangle - \langle \mathbf{g}_k, \mathbf{H}_k \mathbf{p}_k \rangle &= -(1-\rho) \langle \mathbf{g}_k, \tilde{\mathbf{H}}_k \mathbf{p}_k \rangle + \langle \mathbf{g}_k, (\tilde{\mathbf{H}}_k - \mathbf{H}_k) \mathbf{p}_k \rangle \\ &\geq (1-\rho)(1-\theta) \|\mathbf{g}_k\|^2 - \frac{\epsilon}{\tilde{\gamma}} \|\mathbf{g}_k\|^2, \end{aligned}$$

which in turn gives us the lower bound of the right side of inequality (27)

$$\frac{2 \left(\rho \langle \mathbf{g}_k, \tilde{\mathbf{H}}_k \mathbf{p}_k \rangle - \langle \mathbf{g}_k, \mathbf{H}_k \mathbf{p}_k \rangle \right)}{L(\mathbf{x}_0) \|\mathbf{p}_k\|^2} \geq \frac{2\tilde{\gamma}^2}{L(\mathbf{x}_0)} \left((1-\rho)(1-\theta) - \frac{\epsilon}{\tilde{\gamma}} \right).$$

Therefore, line-search will return a step-size, which satisfies

$$\alpha_k \geq \frac{2\tilde{\gamma}^2}{L(\mathbf{x}_0)} \left((1-\rho)(1-\theta) - \frac{\epsilon}{\tilde{\gamma}} \right).$$

So it follows that

$$\begin{aligned}\|\mathbf{g}_{k+1}\|^2 &\leq (1 - 2\alpha_k\rho(1 - \theta))\|\mathbf{g}_k\|^2, \\ &\leq \left(1 - \frac{4\rho\tilde{\gamma}^2(1 - \theta)}{L(\mathbf{x}_0)} \left((1 - \rho)(1 - \theta) - \frac{\epsilon}{\tilde{\gamma}}\right)\right)\|\mathbf{g}_k\|^2.\end{aligned}$$

□

Remark 6. Note that when $\theta = 1 - \tilde{\nu}$, Theorems 4 and 6 exactly coincide.

Similar to Theorem 5, we can obtain error recursion for the case where $\alpha_k = 1$, which can then be used to obtain local problem-independent convergence rate similar to Remark 5.

Theorem 7 (Error Recursion of Algorithm 1 With $\alpha_k = 1$ and Inexact Updates). *Under the assumptions of Theorem 6 with Assumption 3 replaced with (16b), for the iterates of Algorithm 1 with $\alpha_k = 1$ and inexact updates (6), we have*

$$\|\mathbf{g}(\mathbf{x}_{k+1})\| \leq \frac{L_{\mathbf{H}}}{2\tilde{\gamma}^2} \|\mathbf{g}(\mathbf{x}_k)\|^2 + \left(\frac{\epsilon}{\tilde{\gamma}} + \sqrt{2\theta}\right) \|\mathbf{g}(\mathbf{x}_k)\|.$$

where $L_{\mathbf{H}}$, $\tilde{\gamma}$ and θ are, respectively, as in (16b), Lemma 4, and Condition 2.

Proof. Similar to the proof of Theorem 5, using (29b), we have

$$\begin{aligned}\|\mathbf{g}(\mathbf{x}_{k+1})\| &= \|\mathbf{g}(\mathbf{x}_k + \mathbf{p}_k)\| \\ &= \left\| \mathbf{g}(\mathbf{x}_k) + \int_0^1 \mathbf{H}(\mathbf{x}_k + t\mathbf{p}_k)\mathbf{p}_k dt \right\| \\ &= \left\| \mathbf{g}(\mathbf{x}_k) + \tilde{\mathbf{H}}(\mathbf{x}_k)\mathbf{p}_k - \tilde{\mathbf{H}}(\mathbf{x}_k)\mathbf{p}_k + \int_0^1 \mathbf{H}(\mathbf{x}_k + t\mathbf{p}_k)\mathbf{p}_k dt \right\| \\ &\leq \left\| -\tilde{\mathbf{H}}(\mathbf{x}_k)\mathbf{p}_k + \int_0^1 \mathbf{H}(\mathbf{x}_k + t\mathbf{p}_k)\mathbf{p}_k dt \right\| + \left\| \mathbf{g}(\mathbf{x}_k) + \tilde{\mathbf{H}}(\mathbf{x}_k)\mathbf{p}_k \right\| \\ &\leq \|\mathbf{p}_k\| \int_0^1 \|\mathbf{H}(\mathbf{x}_k + t\mathbf{p}_k) - \tilde{\mathbf{H}}(\mathbf{x}_k)\| dt + \epsilon \|\mathbf{p}_k\| + \sqrt{2\theta} \|\mathbf{g}(\mathbf{x}_k)\| \\ &\leq \frac{L_{\mathbf{H}}}{2\tilde{\gamma}^2} \|\mathbf{g}(\mathbf{x}_k)\|^2 + \left(\frac{\epsilon}{\tilde{\gamma}} + \sqrt{2\theta}\right) \|\mathbf{g}(\mathbf{x}_k)\|.\end{aligned}$$

□

Just as in Section 3.4.1, we can also state both Theorems 6 and 7 for the special case of inherently-stable perturbations, which we omit for brevity.

4 Numerical Experiments

In this section, we empirically verify the theoretical results of this paper and also evaluate the performance of Newton-MR as compared with several optimization methods. In particular, we first study the effect of unstable perturbations with $\nu < 1$ in Section 4.1 and show that, somewhat unintuitively, reducing the perturbations indeed results in worsening of the performance. We then turn our attention to two class of problems where $\nu = 1$ and demonstrate that such inherent stability allows for the design of a highly efficient variant of Newton-MR in which the Hessian is suitably approximated.

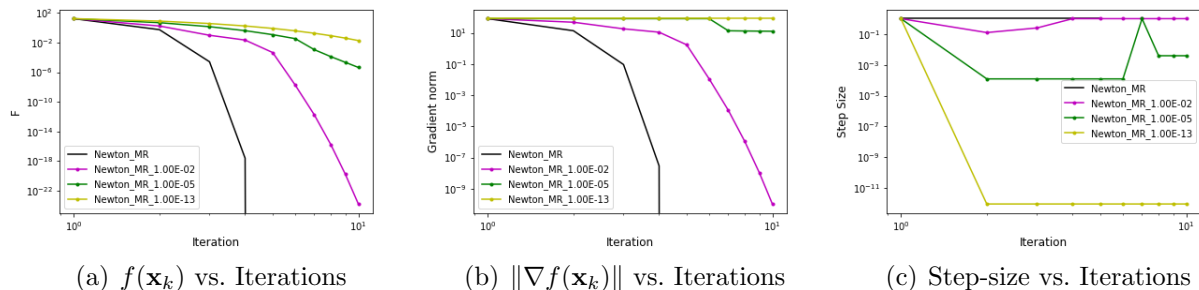


Figure 1: Performance of Newton-MR under an unstable perturbation for $\epsilon = 10^{-2}\gamma$, $10^{-5}\gamma$, and $10^{-13}\gamma$ as described in Section 4.1, e.g., “Newton-MR_1.00E-02” refers to the perturbation with $\epsilon = 10^{-2}\gamma$. “Newton-MR” refers to exact unperturbed algorithm.

4.1 Unstable Perturbations

We now verify the theoretical results of this paper in case of unstable perturbations where $\nu < 1$ and the perturbation is not acute. For this, we consider a simple two dimensional function, taken from [48, Example 5], as

$$f(x_1, x_2) = \frac{ax_1^2}{b - x_2}, \quad (33)$$

where $\text{dom}(f) = \{(x_1, x_2) \mid x_1 \in \mathbb{R}, x_2 \in (-\infty, b) \cup (b, \infty)\}$. Clearly, f is unbounded below and, admittedly, this example is of little interest in optimization. In fact, applying Algorithm 1 to (33) amounts to finding its stationary points, which are of the form $(0, x_2) \in \text{dom}(f)$. Nonetheless, (33) serves our purpose of demonstrating the effects of unstable perturbations in the performance of Algorithm 1.

In [48, Example 5], it has been shown that $\nu = 8/9$. Here, we consider $a = 100, b = 1$ and \mathbf{x}_0 is chosen randomly from standard normal distribution. We construct a noise matrix $\mathbf{E} = \epsilon \mathbf{I}$ and form the perturbed Hessian as $\tilde{\mathbf{H}} = \mathbf{H} + \mathbf{E}$. We consider Algorithm 1 with exact updates for unperturbed as well as perturbed Hessian with $\epsilon = 10^{-2}\gamma, 10^{-5}\gamma$ and $10^{-13}\gamma$, respectively, where $\gamma = \sigma_{\min}(\mathbf{H})$. As seen in Figure 1, for such an unstable perturbation, smaller values of ϵ amount to search directions that, perhaps unintuitively, cease to yield descent in the norm of the gradient, which result

Newton-MR	Newton-CG	Gauss-Newton	ssNewton-MR	ssNewton-CG	L-BFGS
$2(t + \ell + 1)$	$2t + \ell + 2$	$2t + \ell + 2$	$2ts/n + 2(\ell + 1)$	$2ts/n + \ell + 2$	$2(\ell + 1)$
Momentum	Adagrad	Adadelta	RMSprop	Adam	SGD
$2b/n$	$2b/n$	$2b/n$	$2b/n$	$2b/n$	$2b/n$

Table 1: Complexity measure for each iteration of the algorithms for a finite-sum minimization problem involving n functions. Sub-sampled variants of Newton-MR and Newton-CG are referred to, respectively as “ssNewton-MR” and “ssNewton-CG”. We also use t and ℓ to denote, respectively, the total number of iterations for the corresponding inner solver and the line-search. The sample size for estimating the Hessian is denoted by s , whereas b refers the mini-batch size for first order methods.

in the step-size shrinking to zero. These numerical observations reaffirm the theoretical results of Section 3.4.

4.2 Stable Perturbations

In this section, we demonstrate the efficiency of Algorithm 1 under inherently stable perturbations. Our empirical evaluations of this section are done in the context of finite-sum minimization (cf. Example 1). We first make comparisons among several Newton-type methods. In particular, we consider Newton-MR, Newton-CG, as well as their stochastic variants in which the Hessian matrix is sub-sampled. We also consider the classical Gauss-Newton as well as L-BFGS. We then turn our attention to comparison among sub-sampled Newton-MR and several stochastic first-order alternatives in which the gradient is computed only using mini-batches, namely SGD with and without momentum [59], Adagrad [26], RMSProp [60], Adam [34], and Adadelta [66].

Complexity Measure. In all of our experiments, in addition to “wall-clock” time, we consider total number of oracle calls of function, gradient and Hessian-vector product as a complexity measure for evaluating the performance of each algorithm. Similar to [48, Section 4], this is a judicious decision as measuring “wall-clock” time can be highly affected by particular implementation details. The number of such oracle calls for all algorithms considered here is given in Table 1.

Parameters. Throughout this section, we set the maximum iterations of the underlying inner solver, e.g., MINRES-QLP or CG, to 200 with an inexact tolerance of $\theta = 10^{-2}$. In Algorithm 1, we set $\tau = 10^{-10}$ for the termination criterion. The Armijo line-search parameter is set to $\rho = 10^{-4}$, while the parameter of the strong Wolfe curvature condition, used for L-BFGS, is 0.4. The history size of L-BFGS will be kept at 20 past iterations. In the rest of this section, all methods are always initialized at $\mathbf{x}_0 = \mathbf{0}$. For Newton-type methods, the initial trial step-size in line-search is always taken to be one. The step-size of first order methods can be found in Table 2.

Problem	Momentum	Adagrad	Adadelta	RMSprop	Adam	SGD
Softmax (MNIST)	10^{-5}	10^{-4}	10^{-1}	10^{-5}	10^{-5}	10^{-5}
Softmax (Cifar10)	10^{-7}	10^{-6}	10^{-4}	10^{-6}	10^{-7}	10^{-7}
GMM	10^{-8}	10^{-1}	10	10^{-2}	10^{-2}	10^{-8}

Table 2: Step-sizes used for various first order methods. For all problems, the step-size for each method was chosen after careful fine-tuning to obtain the best performance.

4.2.1 Softmax regression

Here, we consider the softmax cross-entropy minimization problem without regularization. More specifically, we have

$$f(\mathbf{x}) \triangleq \mathcal{L}(\mathbf{x}_1, \mathbf{x}_2, \dots, \mathbf{x}_{C-1}) = \sum_{i=1}^n \left(\log \left(1 + \sum_{c'=1}^{C-1} e^{\langle \mathbf{a}_i, \mathbf{x}_{c'} \rangle} \right) - \sum_{c=1}^{C-1} \mathbf{1}(b_i = c) \langle \mathbf{a}_i, \mathbf{x}_c \rangle \right), \quad (34)$$

where $\{\mathbf{a}_i, b_i\}_{i=1}^n$ with $\mathbf{a}_i \in \mathbb{R}^p$, $b_i \in \{0, 1, \dots, C\}$ denote the training data, C is the total number of classes for each input data \mathbf{a}_i and $\mathbf{x} = (\mathbf{x}_1, \mathbf{x}_2, \dots, \mathbf{x}_{C-1})$. Note that, in this case, we have $d = (C - 1) \times p$. It can be shown that, depending on the data, (34) is either strictly convex or merely weakly convex. In either case, however, it has been shown in [48] that $\nu = 1$, i.e., $\nabla f(\mathbf{x}_k) \in \text{Range}(\nabla^2 f(\mathbf{x}_k))$.

Figures 2 and 3 depict, respectively, the performance of variants of Newton-MR as compared with other Newton-type methods and several first order methods. As it can be seen, all variants of Newton-MR are not only highly efficient in terms of oracle calls, but also they are very competitive in terms of “wall-clock” time. In fact, we can see that sub-sampled Newton-MR converges faster than all first order methods considered here. This can be attributed to moderate per-iteration cost of sub-sampled Newton-MR, which is coupled with far fewer overall iterations.

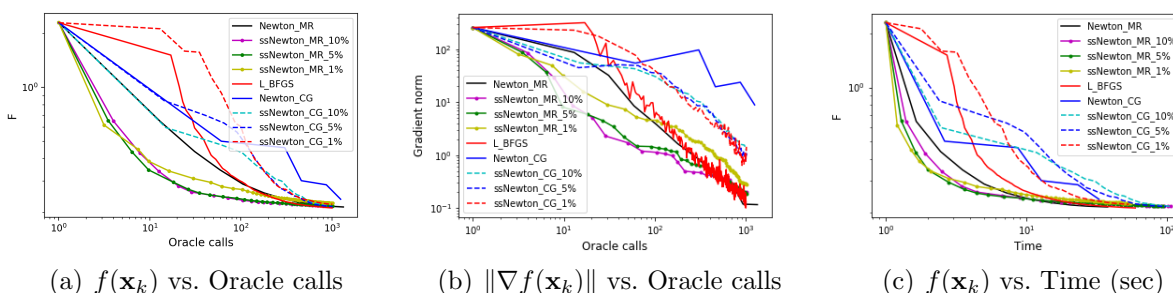


Figure 2: Comparison among Newton-type methods on (34) using MNIST dataset. Here, sample sizes are chosen as $s = 0.1n, 0.05n$ and $0.01n$, e.g., “ssNewton-MR_10%” uses $s = 0.1n$.

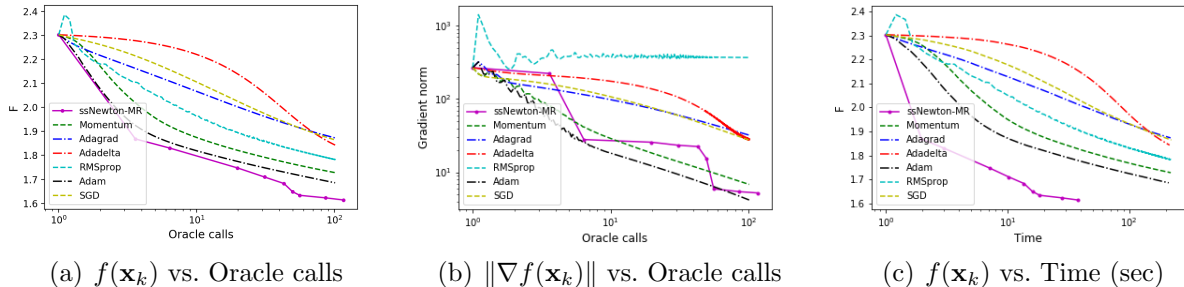


Figure 3: Comparison among sub-sampled Newton-MR and several first order methods on (34) using Cifar10 dataset. Here, sample/mini-batch sizes are $s = b = 0.05n$.

We then compare the performance of Newton-MR and Newton-CG as it relates to sensitivity to Hessian perturbations. We consider full and sub-sampled variants of both algorithms for a range of samples-sizes. Figures 4 and 5 clearly demonstrate that Newton-MR exhibits a great deal of robustness to Hessian perturbations, which amount to better performance for crude Hessian approximations. This is in sharp contrast to Newton-CG, which requires more accurate Hessian estimations to perform comparatively. Note the large variability in the performance of sub-sampled Newton-CG as compared with rather uniform performance of sub-sampled Newton-MR.

4.2.2 Gaussian Mixture Model

Here, we consider an example involving a mixture of Gaussian densities. Although this problem is non-convex, it exhibits features that are close to being convex, e.g, small regions of saddle points and large regions containing global minimum, [39]. For simplicity, we consider a mixture model with two Gaussian components as

$$f(\mathbf{x}) \triangleq \mathcal{L}(w, \mathbf{u}, \mathbf{v}) = - \sum_{i=1}^n \log (\zeta(w)\Phi(\mathbf{a}_i; \mathbf{u}, \Sigma_1) + (1 - \zeta(w)) \Phi(\mathbf{a}_i; \mathbf{v}, \Sigma_2)), \quad (35)$$

where Φ denotes the density of the p -dimensional standard normal distribution, $\mathbf{a}_i \in \mathbb{R}^p$ are the data points, $\mathbf{u}, \mathbf{v} \in \mathbb{R}^p$, $\Sigma_1, \Sigma_2 \in \mathbb{R}^{p \times p}$ are the corresponding mean vectors and the covariance matrices of two the Gaussian distributions, $w \in \mathbb{R}$ and $\zeta(t) = 1/(1+e^{-t})$ is to ensure that the mixing weight lies within $[0, 1]$. Here, one can show that $\nu = 1$. Note that, here, $\mathbf{x} \triangleq [w; \mathbf{u}; \mathbf{v}] \in \mathbb{R}^{2p+1}$. In each run, we generate 1,000 random data points, generated from the mixture distribution (35) with $p = 100$, and ground truth parameters as $w^* \sim \mathcal{N}[0, 1]$, $\mathbf{u}^* \sim \mathcal{N}[-1, 1]$, $\mathbf{v}^* \sim \mathcal{U}[3, 4]$. Covariance matrices are constructed randomly, with controlled condition number, such that they are not axis-aligned. To establish this, we first randomly generate two $p \times p$ matrices whose elements are i.i.d. drawn from standard normal distribution and uniform distribution, respectively. We then find the corresponding orthogonal bases, $\mathbf{Q}_1, \mathbf{Q}_2$, using QR factorization. We then set $\Sigma_i = \mathbf{Q}_i^T \mathbf{D}^{-1} \mathbf{Q}_i$ where \mathbf{D} is a diagonal matrix whose diagonal entries are chosen equidistantly from the interval $[0, 10^8]$. This way the condition

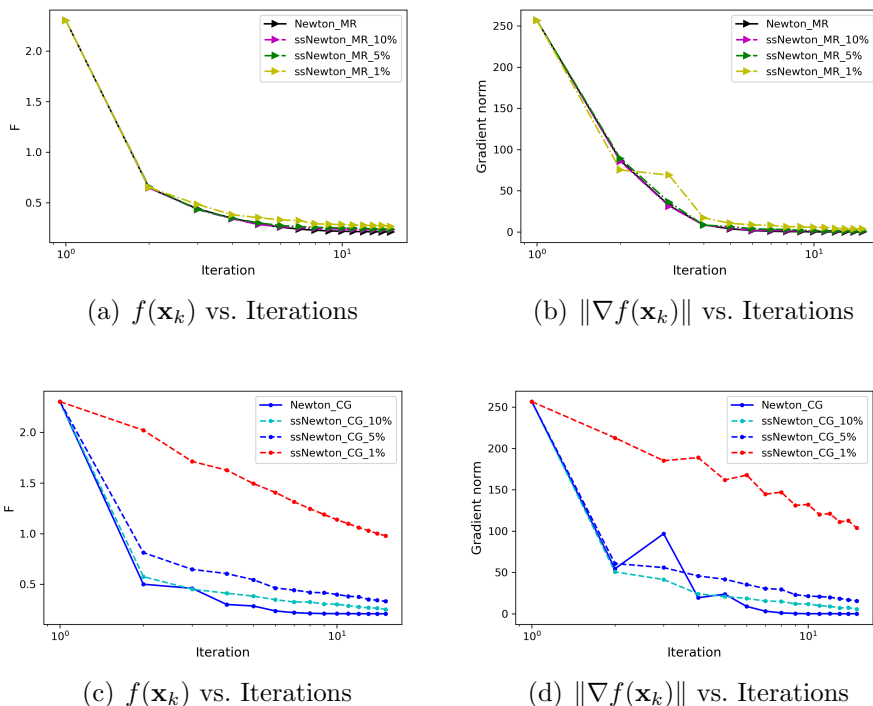


Figure 4: Stability comparison between full and sub-sampled variants of Newton-MR and Newton-CG using $s = 0.1n, 0.05n, 0.01n$ in Table 1 on (34) with MNIST dataset.

number of each Σ_i is 10^8 . In all the figures,

$$\text{Estimation error at } k^{\text{th}} \text{ iteration} \triangleq \frac{1}{2} \left(\frac{|w_k - w^*|}{w^*} + \frac{\|[\mathbf{u}_k; \mathbf{v}_k] - [\mathbf{u}^*; \mathbf{v}^*]\|}{\|[\mathbf{u}^*; \mathbf{v}^*]\|} \right).$$

In our experiments, the classical Gauss-Newton method performed extremely poorly, and as a result we did not consider its sub-sampled variants. Figure 6 shows the performance profile plots [25, 30] with 500 runs for Newton-type methods and Figures 7 and 8 depict the corresponding plots comparing variants of Newton-MR with several first order methods using, respectively, sample/mini-batch sizes of 5% and 1%. Recall that in performance profile plots, for a given λ in the x-axis, the corresponding value on the y-axis is the proportion of times that a given solver’s performance lies within a factor λ of the best possible performance over all runs.

As demonstrated by Figure 6, although L-BFGS performs competitively in terms of reducing the objective function, its performance in terms of parameter recovery and estimation error is far worse than all other methods. In contrast, all variants of Newton-MR have stable performance across all 500 runs, with sub-sampled variants exhibiting superior performance. Figure 7 and 8 also demonstrate similar superior performance compared with first order algorithms.

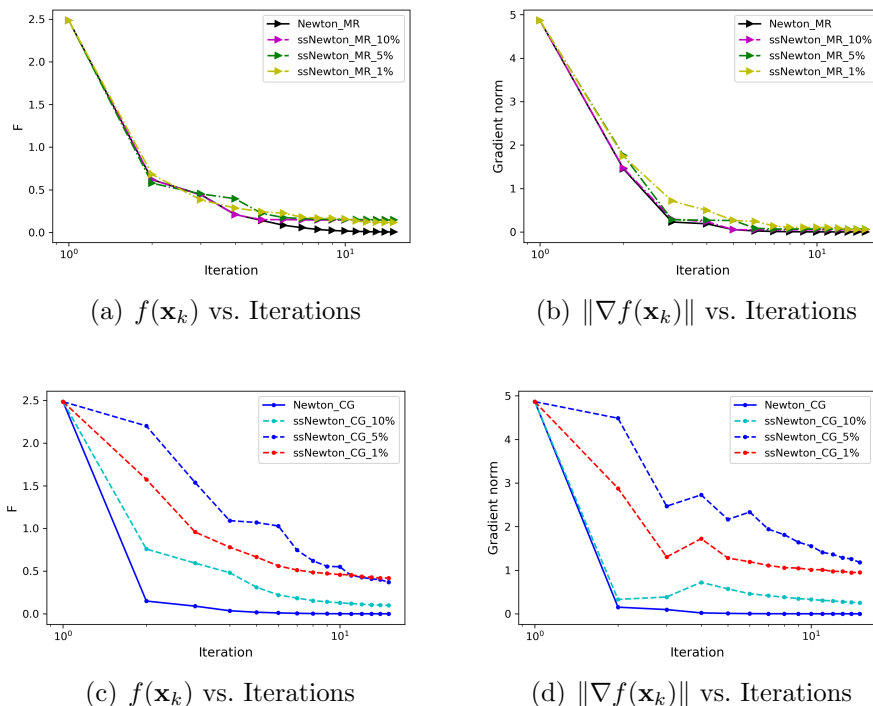


Figure 5: Stability comparison between full and sub-sampled variants of Newton-MR and Newton-CG using $s = 0.1n, 0.05n, 0.01n$ in Table 1 on (34) with HAPT dataset.

5 Conclusions

In this paper, we considered the stability analysis of Newton-MR [48] under Hessian perturbations in the form of additive noise model. It is known that the pseudo-inverse of the Hessian is a discontinuous function of such perturbations. As a result, the pseudo-inverse of the perturbed Hessian can grow unboundedly with diminishing noise. However, our results indicate that it can indeed remain bounded along certain directions and under favorable conditions. We showed that the concept of inherently stable perturbations encapsulates situations under which Newton-MR with noisy Hessian remains stably convergent. Under such conditions, we established global and local convergence results for Algorithm 1 using both exact and inexact updates. We argued that such stability analysis allows for the design of efficient variants of Newton-MR in which curvature information is approximated to reduce the computational costs in large-scale problems. We then numerically demonstrated the validity of our theoretical result and evaluated the performance of several such variants of Newton-MR as compared with various first and second-order methods.

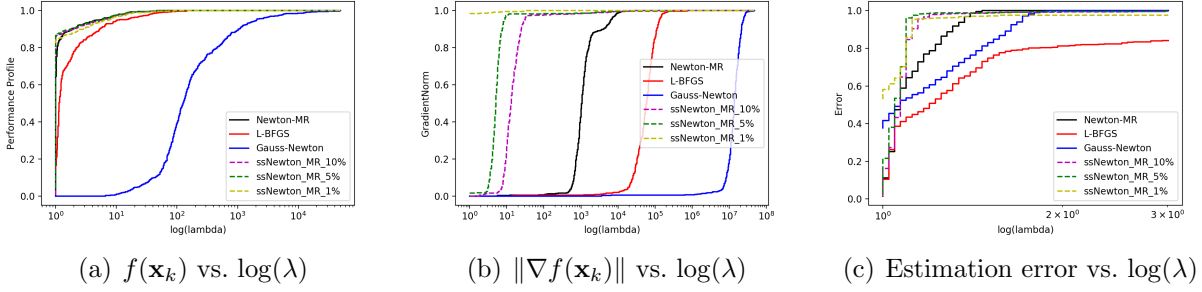


Figure 6: Performance profile for 500 runs of various Newton-type methods for solving (35) as detailed in Section 4.2.2.

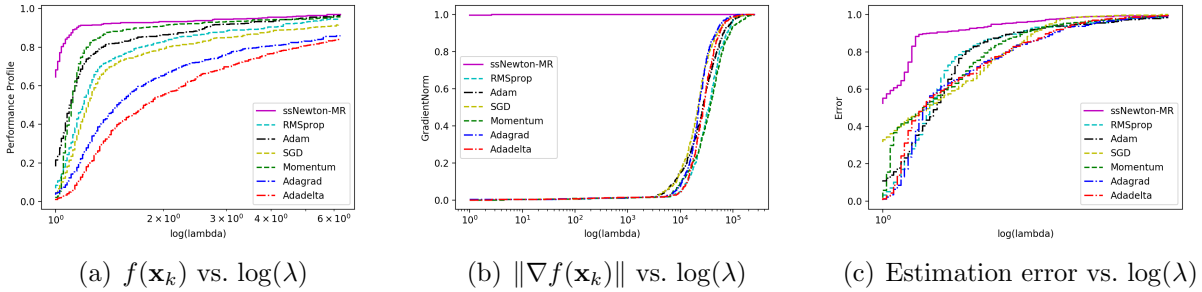


Figure 7: Performance profile for 500 runs of Newton-MR variants and several first-order methods for solving (35) as detailed in Section 4.2.2. Here, we have set $s = b = 0.05n$.

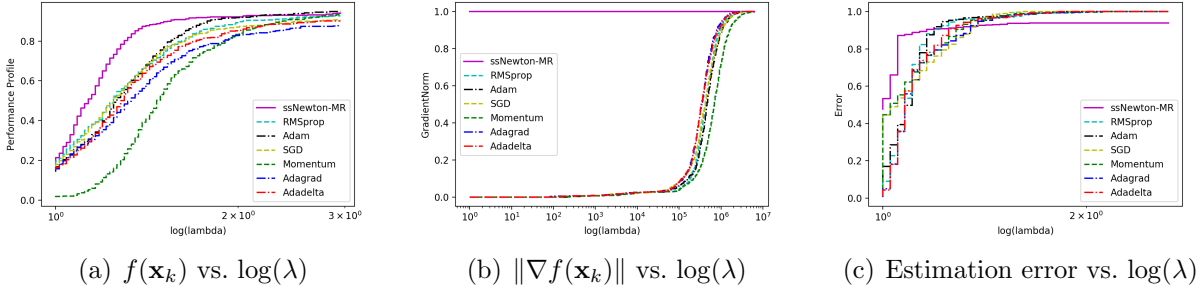


Figure 8: Performance profile for 500 runs of Newton-MR variants and several first-order methods for solving (35) as detailed in Section 4.2.2. Here, we have set $s = b = 0.01n$.

Acknowledgment

All authors are grateful for the support by the Australian Centre of Excellence for Mathematical and Statistical Frontiers (ACEMS). Fred Roosta was partially supported by DARPA as well as the Australian Research Council through a Discovery Early Career Researcher Award (DE180100923).

References

- [1] Larry Armijo et al. Minimization of functions having Lipschitz continuous first partial derivatives. *Pacific Journal of mathematics*, 16(1):1–3, 1966.
- [2] Afonso S Bandeira, Katya Scheinberg, and Luís N Vicente. Convergence of trust-region methods based on probabilistic models. *SIAM Journal on Optimization*, 24(3):1238–1264, 2014.
- [3] Albert S Berahas, Raghu Bollapragada, and Jorge Nocedal. An investigation of Newton-sketch and subsampled Newton methods. *arXiv preprint arXiv:1705.06211*, 2017.
- [4] Dennis S Bernstein. *Matrix Mathematics: Theory, Facts, and Formulas With Application to Linear Systems Theory*, volume 41. Princeton University Press Princeton, 2009.
- [5] Dimitri P. Bertsekas. *Convex Optimization Algorithms*. Athena Scientific Belmont, 2015.
- [6] Jose Blanchet, Coralia Cartis, Matt Menickelly, and Katya Scheinberg. Convergence rate analysis of a stochastic trust region method for nonconvex optimization. *arXiv preprint arXiv:1609.07428*, 2016.
- [7] Raghu Bollapragada, Richard Byrd, and Jorge Nocedal. Exact and Inexact Subsampled Newton Methods for Optimization. *arXiv preprint arXiv:1609.08502*, 2016.
- [8] Stephen Boyd and Lieven Vandenberghe. *Convex optimization*. Cambridge university press, 2004.
- [9] Richard H. Byrd, Gillian M. Chin, Will Neveitt, and Jorge Nocedal. On the use of stochastic Hessian information in optimization methods for machine learning. *SIAM Journal on Optimization*, 21(3):977–995, 2011.
- [10] Richard H. Byrd, Gillian M. Chin, Jorge Nocedal, and Yuchen Wu. Sample size selection in optimization methods for machine learning. *Mathematical programming*, 134(1):127–155, 2012.
- [11] D Calvetti, B Lewis, and L Reichel. GMRES, L-curves, and discrete ill-posed problems. *BIT Numerical Mathematics*, 42(1):44–65, 2002.
- [12] Daniela Calvetti, Bryan Lewis, and Lothar Reichel. L-curve for the MINRES method. In *Advanced Signal Processing Algorithms, Architectures, and Implementations X*, volume 4116, pages 385–396. International Society for Optics and Photonics, 2000.
- [13] Yair Carmon, John C Duchi, Oliver Hinder, and Aaron Sidford. Accelerated methods for non-convex optimization. *arXiv preprint arXiv:1611.00756*, 2016.
- [14] Yair Carmon, John C Duchi, Oliver Hinder, and Aaron Sidford. Convex until proven guilty: Dimension-free acceleration of gradient descent on non-convex functions. In *Proceedings of the 34th International Conference on Machine Learning-Volume 70*, pages 654–663. JMLR. org, 2017.

- [15] C Cartis, N. I. M. Gould, and Philip L. Toint. Adaptive cubic regularisation methods for unconstrained optimization. Part I: motivation, convergence and numerical results. *Mathematical Programming*, 127(2):245–295, 2011.
- [16] C Cartis, N. I. M. Gould, and Philip L. Toint. Adaptive cubic regularisation methods for unconstrained optimization. Part II: worst-case function-and derivative-evaluation complexity. *Mathematical programming*, 130(2):295–319, 2011.
- [17] Coralia Cartis, N. I. M. Gould, and Philip L. Toint. Complexity bounds for second-order optimality in unconstrained optimization. *Journal of Complexity*, 28(1):93–108, 2012.
- [18] Ruobing Chen, Matt Menickelly, and Katya Scheinberg. Stochastic optimization using a trust-region method and random models. *arXiv preprint arXiv:1504.04231*, 2015.
- [19] Sou-Cheng T Choi, Christopher C Paige, and Michael A Saunders. MINRES-QLP: A Krylov subspace method for indefinite or singular symmetric systems. *SIAM Journal on Scientific Computing*, 33(4):1810–1836, 2011.
- [20] Sou-Cheng T Choi and Michael A Saunders. Algorithm 937: MINRES-QLP for symmetric and Hermitian linear equations and least-squares problems. *ACM Transactions on Mathematical Software (TOMS)*, 40(2):16, 2014.
- [21] P.G. Ciarlet. *Linear and Nonlinear Functional Analysis with Applications*. Society for Industrial and Applied Mathematics, 2013.
- [22] Andrew R Conn, N. I. M. Gould, and Philip L. Toint. *Trust region methods*, volume 1. SIAM, 2000.
- [23] Andrew R Conn, Katya Scheinberg, and Luís N Vicente. Global convergence of general derivative-free trust-region algorithms to first-and second-order critical points. *SIAM Journal on Optimization*, 20(1):387–415, 2009.
- [24] CY Deng and Yimin Wei. Perturbation analysis of the Moore-Penrose inverse for a class of bounded operators in Hilbert spaces. *J. Korean Math. Soc*, 47(4):831–843, 2010.
- [25] Elizabeth D Dolan and Jorge J Moré. Benchmarking optimization software with performance profiles. *Mathematical programming*, 91(2):201–213, 2002.
- [26] John Duchi, Elad Hazan, and Yoram Singer. Adaptive subgradient methods for online learning and stochastic optimization. *The Journal of Machine Learning Research*, 12:2121–2159, 2011.
- [27] Murat A. Erdogdu and Andrea Montanari. Convergence rates of sub-sampled Newton methods. In *Advances in Neural Information Processing Systems 28*, pages 3034–3042. 2015.
- [28] David Chin-Lung Fong and Michael Saunders. CG versus MINRES: An empirical comparison. *Sultan Qaboos University Journal for Science [SQUJS]*, 17(1):44–62, 2012.
- [29] G.H. Golub and C.F. Van Loan. *Matrix Computations*. Johns Hopkins Studies in the Mathematical Sciences. Johns Hopkins University Press, 4 edition, 2012.

- [30] Nicholas Gould and Jennifer Scott. A note on performance profiles for benchmarking software. *ACM Transactions on Mathematical Software (TOMS)*, 43(2):15, 2016.
- [31] Gratton, Serge and Royer, Clément W and Vicente, Luís N and Zhang, Zaikun. Complexity and global rates of trust-region methods based on probabilistic models. *IMA Journal of Numerical Analysis*, 38(3):1579–1597, 2018.
- [32] Martin Hanke. *Conjugate gradient type methods for ill-posed problems*. Routledge, 2017.
- [33] John H Hubbard and Barbara Burke Hubbard. *Vector Calculus, Linear Algebra, and Differential Forms*. Matrix Editions, 5th edition, 2015.
- [34] Diederik P Kingma and Jimmy Ba. Adam: A method for stochastic optimization. *arXiv preprint arXiv:1412.6980*, 2014.
- [35] Sudhir Kylasa, Farbod Roosta-Khorasani, Michael W Mahoney, and Ananth Grama. GPU Accelerated Sub-Sampled Newton’s Method for Convex Classification Problems. In *Proceedings of the 2019 SIAM International Conference on Data Mining*, pages 702–710. SIAM, 2019.
- [36] Jeffrey Larson and Stephen C Billups. Stochastic derivative-free optimization using a trust region framework. *Computational Optimization and Applications*, 64(3):619–645, 2016.
- [37] Kenneth Levenberg. A method for the solution of certain problems in least squares. *Quarterly of Applied Mathematics*, 2(2):164–168, 1944.
- [38] Donald W Marquardt. An algorithm for least-squares estimation of nonlinear parameters. *Journal of the Society for Industrial & Applied Mathematics*, 11(2):431–441, 1963.
- [39] Song Mei, Yu Bai, and Andrea Montanari. The landscape of empirical risk for non-convex losses. *arXiv preprint arXiv:1607.06534*, 2016.
- [40] Lingsheng Meng and Bing Zheng. The optimal perturbation bounds of the Moore–Penrose inverse under the Frobenius norm. *Linear Algebra and its Applications*, 432(4):956–963, 2010.
- [41] Shashi K Mishra and Giorgio Giorgi. *Inverity and Optimization*, volume 88. Springer Science & Business Media, 2008.
- [42] Yurii Nesterov. *Introductory lectures on convex optimization*, volume 87. Springer Science & Business Media, 2004.
- [43] Yurii Nesterov and Boris T Polyak. Cubic regularization of Newton method and its global performance. *Mathematical Programming*, 108(1):177–205, 2006.
- [44] Jorge Nocedal and Stephen Wright. *Numerical optimization*. Springer Science & Business Media, 2006.
- [45] Sean O’Rourke, Van Vu, and Ke Wang. Random perturbation of low rank matrices: Improving classical bounds. *Linear Algebra and its Applications*, 540:26–59, 2018.

- [46] Christopher C Paige and Michael A Saunders. Solution of sparse indefinite systems of linear equations. *SIAM journal on numerical analysis*, 12(4):617–629, 1975.
- [47] Mert Pilanci and Martin J. Wainwright. Newton Sketch: A Linear-time Optimization Algorithm with Linear-Quadratic Convergence. *arXiv preprint arXiv:1505.02250*, 2015.
- [48] Fred Roosta, Yang Liu, Peng Xu, and Michael W Mahoney. Newton-MR: Newton’s Method Without Smoothness or Convexity. *arXiv preprint arXiv:1810.00303*, 2018.
- [49] Farbod Roosta-Khorasani and Michael W Mahoney. Sub-sampled Newton methods I: globally convergent algorithms. *arXiv preprint arXiv:1601.04737*, 2016.
- [50] Farbod Roosta-Khorasani and Michael W. Mahoney. Sub-sampled Newton methods. *Mathematical Programming*, 174(1):293–326, 2019.
- [51] Farbod Roosta-Khorasani and Michael W Mahoney. Sub-sampled Newton methods. *Mathematical Programming*, 174(1-2):293–326, 2019.
- [52] Clément W Royer, Michael O’Neill, and Stephen J Wright. A Newton-CG algorithm with complexity guarantees for smooth unconstrained optimization. *Mathematical Programming*. <https://doi.org/10.1007/s10107-019-01362-7>.
- [53] Clément W Royer and Stephen J Wright. Complexity analysis of second-order line-search algorithms for smooth nonconvex optimization. *SIAM Journal on Optimization*, 28(2):1448–1477, 2018.
- [54] Mark Rudelson and Roman Vershynin. Non-asymptotic theory of random matrices: extreme singular values. In *Proceedings of the International Congress of Mathematicians 2010 (ICM 2010) (In 4 Volumes) Vol. I: Plenary Lectures and Ceremonies Vols. II–IV: Invited Lectures*, pages 1576–1602. World Scientific, 2010.
- [55] Sara Shashaani, Fatemeh Hashemi, and Raghu Pasupathy. ASTRO-DF: A Class of Adaptive Sampling Trust-Region Algorithms for Derivative-Free Stochastic Optimization. *arXiv preprint arXiv:1610.06506*, 2016.
- [56] Gilbert W Stewart. On the perturbation of pseudo-inverses, projections and linear least squares problems. *SIAM review*, 19(4):634–662, 1977.
- [57] GW Stewart. Rank degeneracy. *SIAM Journal on Scientific and Statistical Computing*, 5(2):403–413, 1984.
- [58] G.W. Stewart and Ji guang Sun. *Matrix Perturbation Theory*. Academic Press, 1990.
- [59] Ilya Sutskever, James Martens, George Dahl, and Geoffrey Hinton. On the importance of initialization and momentum in deep learning. In *International conference on machine learning*, pages 1139–1147, 2013.
- [60] Tijmen Tieleman and Geoffrey Hinton. Lecture 6.5-rmsprop: Divide the gradient by a running average of its recent magnitude. *COURSERA: Neural Networks for Machine Learning*, 4, 2012.
- [61] Per-Åke Wedin. Perturbation theory for pseudo-inverses. *BIT Numerical Mathematics*, 13(2):217–232, 1973.

- [62] Peng Xu, Farbod Roosta-Khorasani, and Michael W. Mahoney. Second-Order Optimization for Non-Convex Machine Learning: An Empirical Study. *arXiv preprint arXiv:1708.07827*, 2017.
- [63] Peng Xu, Farbod Roosta-Khorasani, and Michael W Mahoney. Newton-type methods for non-convex optimization under inexact Hessian information. *Mathematical Programming*, 2019. doi:10.1007/s10107-019-01405-z.
- [64] Peng Xu, Jiyan Yang, Farbod Roosta-Khorasani, Christopher Ré, and Michael W Mahoney. Sub-sampled newton methods with non-uniform sampling. In *Advances in Neural Information Processing Systems*, pages 3000–3008, 2016.
- [65] Zhewei Yao, Peng Xu, Farbod Roosta-Khorasani, and Michael W Mahoney. Inexact non-convex Newton-type methods. *arXiv preprint arXiv:1802.06925*, 2018.
- [66] Matthew D Zeiler. ADADELTA: an adaptive learning rate method. *arXiv preprint arXiv:1212.5701*, 2012.